REPUBLIC OF TURKEY

ALTINBAŞ UNIVERSITY

Institute of Graduate Studies

Information Technology

DESIGN AND SIMULATION OF TUNABLE MICROSTRIP ANTENNA FOR 5G NETWORKS

Omer ABDULRAZAQ

Master's Thesis

Supervisor

Prof. Dr. Oguz BAYAT

Istanbul, 2022

DESIGN AND SIMULATION OF TUNABLE MICROSTRIP ANTENNA FOR 5G NETWORKS

Omer ABDULRAZAQ

Information Technology

Master’s Thesis

ALTINBAŞ UNIVERSITY

2022

The thesis titled “DESIGN AND SIMULATION OF TUNABLE MICROSTRIP ANTENNA FOR 5G NETWORKS” prepared by OMER ABDULRAZAQ and submitted on 22/10/2021 has been **accepted unanimously** for the degree of Master of Science in Information Technology.

Prof. Dr. Oguz BAYAT

Supervisor

Thesis Defense Committee Members:

Prof. Dr. Oguz BAYAT	Faculty of Engineering and Architecture, Altınbaş University	_____
Asst. Prof. Muhammad ILYAS	Faculty of Engineering and Architecture, Altınbaş University	_____
Asst. Prof. Adil DENİZ	Biomedical Engineering and Technology, Marmara University	_____

I hereby declare that this thesis meets all format and submission requirements of a Master’s thesis.

Accepted by Altınbaş University Institute of Graduate Studies on the following date:

____/____/____

I hereby declare that all information/data presented in this graduation project has been obtained in full accordance with academic rules and ethical conduct. I also declare all unoriginal materials and conclusions have been cited in the text and all references mentioned in the Reference List have been cited in the text, and vice versa as required by the abovementioned rules and conduct.

Omer ABDULRAZAQ

Signature

ABSTRACT

DESIGN AND SIMULATION OF TUNABLE MICROSTRIP ANTENNA FOR 5G NETWORKS

Abdulrazaq, Omer

M.Sc, Information Technology, Altınbaş University,

Supervisor: Asst. Prof. Dr. Oguz BAYAT

Date: May/2021

Pages: 61

With the recent development in the communication technology and increase the connected machines (things) in the network the congestion happen which lead to minimising the data rate. So, the operators newly placed the base for the 5G and already begin in some countries by utilising the higher frequencies (e.g. 28GHz). One of the most popular antenna types is the microstrip antennas which is characterised by their small size and agile weight which make them compatible to operate in the 5G networks. On the other hand, these antennas endure some issues such as the poor gain and the tight bandwidth. In this work, a rectangular microstrip patch antenna (RMPA) with two implant graphene flakes is simulated and optimised base on the CST antenna simulation software. The flakes of the graphene material are helping to reconfigure the frequency based on the applied voltage that leads to variate its surface impedance where the flake impedance minimised once the applied voltage increased and vice-versa. Thus, resulting in a shift in the operating frequency. In order to improve the performance, the array structure is utilised to increase the antenna gain. The proposed antenna operates in the range of frequency about (27.75- 29.4 GHz) with a gain (6.12-4.99 dBi) for the single antenna element. While for the array configuration the frequency is about the range of (27.95-28.84 GHz) and the gain is about (11 dBi).

Keywords: 5G, Microstrip Patch Antenna, 28GHz, CST, Graphene.

TABLE OF CONTENTS

Pages

LIST OF TABLES

Pages

LIST OF FIGURES

Pages

ABBREVIATIONS

1G	:	First Generation
2G	:	Second Generation
3G	:	Third Generation
4G	:	Fourth Generation
5G	:	Fifth Generation
BW	:	Bandwidth
CST	:	Computer Simulation Technology
GPS	:	Global Positioning System
GSM	:	Global System for Mobile
LOS	:	Line of Sight
MA	:	Microstrip Antenna
NLOS	:	Non-Line of Sight
NTT	:	Nippon Telephone and Telegraph”
RL	:	Return Loss
RMPA	:	Rectangular Microstrip Patch Antenna
RMPAA	:	Rectangular Microstrip Patch Antenna Array
Wi-Fi	:	Wireless Fidelity

1. INTRODUCTION

1.1 GENERAL INTRODUCTION

This chapter consists of many of the subsections that covers the wireless networks, evolution of the wireless communications, millimetre waves (mm-Waves), propagation properties of mm-Waves, applications of mm-Waves, literature survey, problem statement, thesis objectives, and thesis outline.

1.2 WIRELESS NETWORKS

Wireless networks are called computer networks that are not cable-connected. They usually employ the radio waves to connect the network nodes. The users are able to connect their things to the network while roaming around the network, as illustrated in Figure 1.1. With a wireless network, devices can remain connected to the network without any wiring. Access points enhance Wi-Fi, allowing a device to be far away from a router, but still connected to the network. If a hotel, a hotel, an airport lounge or another public space is connected to the Wi-Fi hotspot you are connected to the wireless Internet of the company [1].

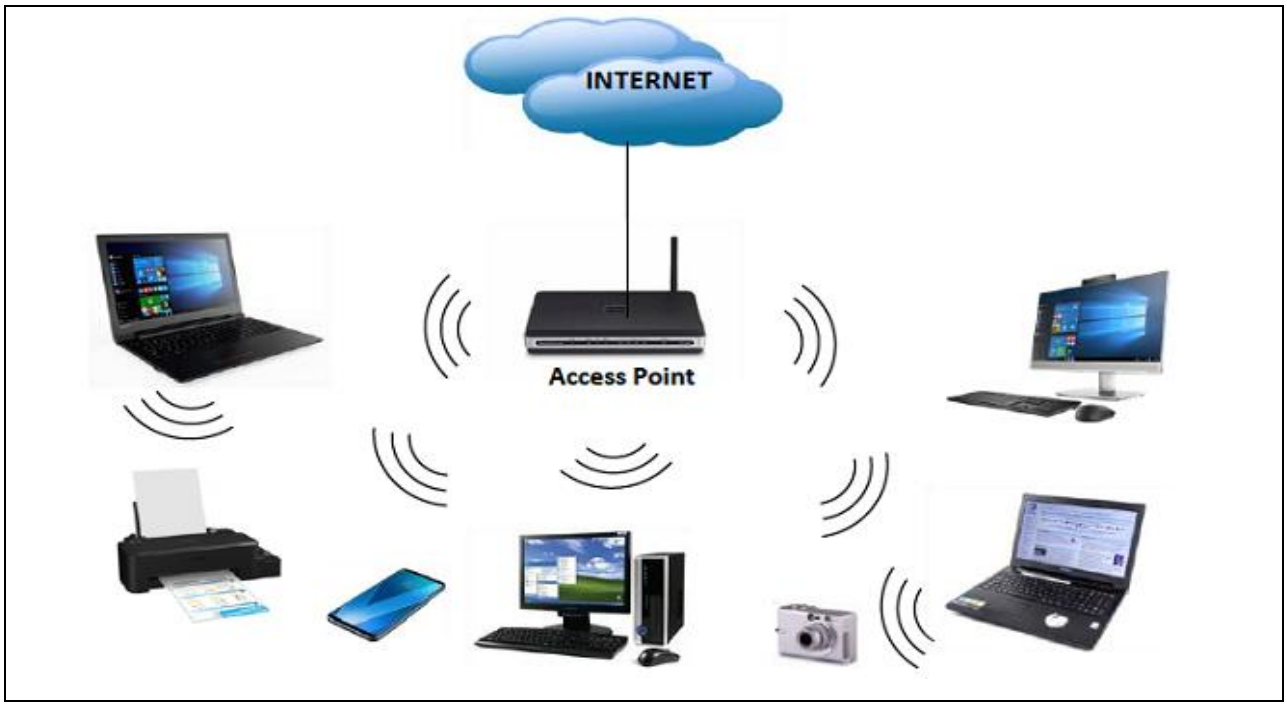

Figure 1.1: Devices Connection with The Network [1].

In a wired network, cables can be connected to the Internet or to another network, for example, laptop or desktop computers. Compared to a wireless network, a wired network has some disadvantages. Your device is tied up to a router the biggest disadvantage. Cables connected to an Ethernet port on one end of the network router, and to a computer or other device are used by the most common wired networks. In order to create the wireless network, the users are able to select among a three known types of deployment: the centralised, the converged deployment, and the cloud-based deployment [2].

1.3 EVOLUTION OF WIRELESS COMMUNICATIONS

In the last few decades after the first generation ($1G$) the mobile network was launched in the early 1980s, mobile wireless communication has undergone several developmental phases. Mobile communication standards have quickly advanced to support more extra users due to the large request for more extra connections around the world. This section covers the evolutionary phases of mobile communication wireless technologies. In the 1895, an inventor from the Italy, called as Marconi is wirelessly transmitted code signs from Morse practising the radio waves for 3.2 km. It was in science's history the first wireless transmission. Efficient communication with RF waves has since been worked out by engineers and scientists. In the middle of the 19th century, the telephone became popular. Thanks to the wired connection and reduced mobility, engineers have started to develop a device that does not need wired connectivity. The Nippon Telephone and Telegraph Company (NTT) deployed its 1G of mobile networks in Japan in Tokyo in 1979. The United States, Finland, UK and Europe became more popular in the early 1980s. The system used analogue signals, and because of technological limitations, had many disadvantages. However, a range of inconveniences affected 1G technology. The coverage was a pauper and the quality of the sound was depressed. Also, the 1G was unable to the roaming support was available among different network company operators, and there was no compatibility among the systems since different systems work in distinct frequency ranges. Worse than that, calls were not encrypted, so anybody could make a call with a radio scanner. However, a range of inconveniences affected 1G technology. The coverage was a pauper and the quality of the sound was depressed. Also, the 1G was unable to the roaming support was available among different network company operators, and there was no compatibility among the systems since different systems work in distinct frequency ranges [3]. Worse than that, calls were not encrypted, so anybody could make a call with a radio

scanner. In addition, its utilisation was limited for applying the voice calls. Another mobile network that followed the 1G is the second generation (2G) was originated in Finland in 1991 beneath the GSM standard. In this generation, the calls can be encrypted for the first time and digital voice calls with less calm and the background cracking were safely more clearly. The 2G was extremely longer than telecommunications; it contributed to laying the foundations for the cultural reconstruction. For the first time, on their phones, people could send text messages, images and multimedia. The analogue history of the 1G led to the presentation of 2G's digital future [4]. This led to mass adoption, on a scale never before observed, by users and companies alike. After the emerging of the 2G followed that the starting of the third generation (3G) was originated in 2001 with the objective of standardizing the vendor's network protocol. This indicated that users able to accessing the web connectivity data from anywhere in the world as the "data-packets." For the first time, this presented it a real opportunity for international roaming services. Expanded the capacity for data transfer by 3G (4 times than that in the 2G) headed to the increase of new services like video conferencing, video and voice through IP (such as Skype). Followed the 3G In 2009, the fourth generation (4G) was first used as the Long-Term Evolution (LTE) 4G standard for Stockholm, Sweden and Oslo, Norway. It was later submitted around the world and became an actuality for millions of consumers through high-quality video streaming. The 4G provides fast mobile web entrance to the gaming services, high definition and high-quality video conferencing (up to 1 Gb/s for the permanent users). As a result, mobile devices demanded designed to carry the 4G while switching from the 2G to the 3G were as simple as switching SIM cards. In the recent past, the next objective has been to implement the 5th generation, with the provision of a higher data rate required to start in 2020. With increasing network applications and data rate demands today, the only option available to wireless technology operators is to switch to higher frequencies to avoid data congestion. Like these bands, the data rates are higher and the spectrum efficiency required at present. Real gigabytes are required to be in the range between 30 and 300 GHz in a millimetre (mm) wavelength. The advancement of the wireless communications operations is illustrated in Figure 1.2. Due to its potential functional benefits for several later utilisation, such frequency band has achieved greater excitement and recognition for the researchers. The formulation of new technologies in this frequency band has led to numerous of the high-speed wireless like the video streaming, high-speed internet, multimedia interfaces, wireless gigabit ethernet and automotive radar [5].

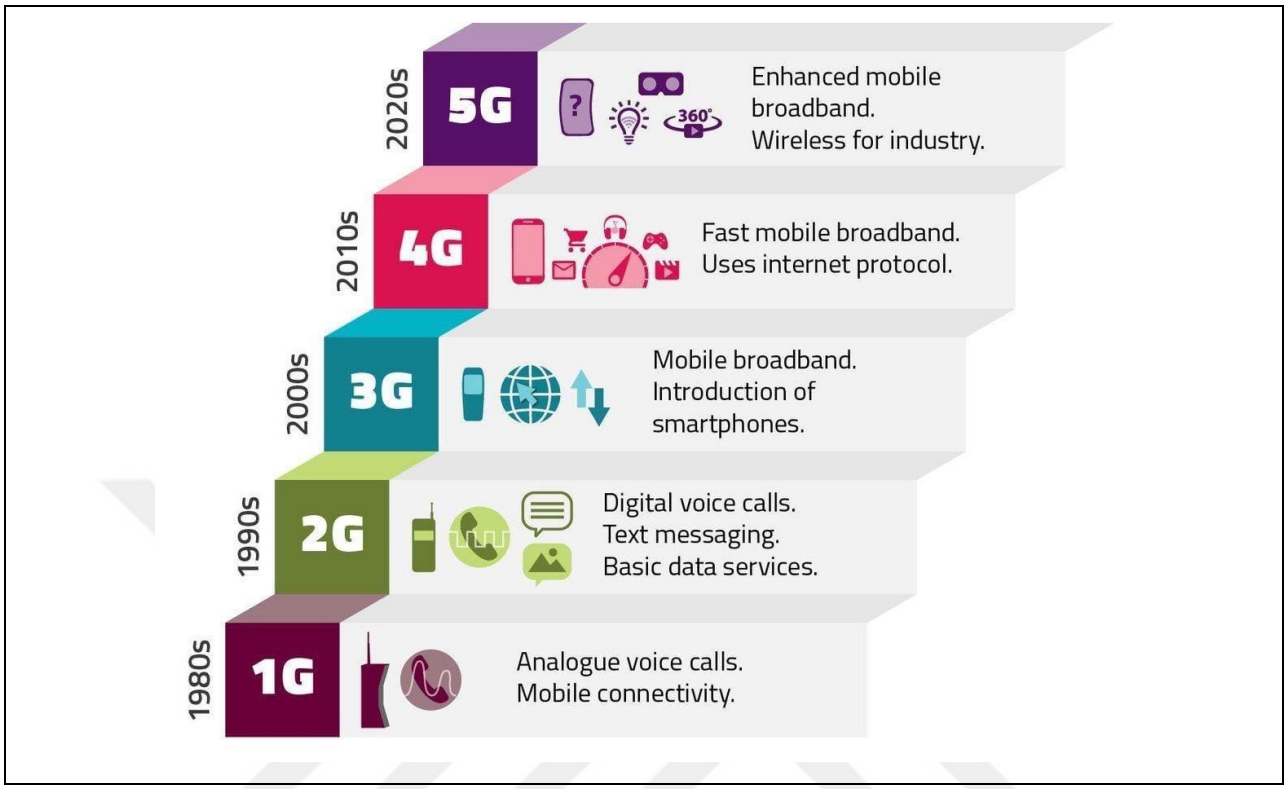

Figure 1.2: Evolution of Wireless Communications [5].

1.4 IMPORTANCE OF WIRELESS COMMUNICATIONS

As was mentioned earlier, the majority of today's modern telecommunication is conducted over wireless networks. It is the process of transmitting data over a relatively short distance or across the entire earth without the utilization of wires, cables, or any other form of electrical conductors. Wireless communications are soaring to new heights thanks to the proliferation of various commercial interests. The advent of wireless technology has brought about improvements in network productivity, adaptability, and velocity. Because it facilitates the simple exchange of information and boosts productivity, it has developed into a useful instrument for the generation that is well versed in technology. The advent of wireless communications has made it possible for people to travel to any location they choose without having to worry about losing their ability to stay connected to the internet. Wireless communications have made it possible for billions of people to connect to the Internet, which has enabled them to participate in the digital economy of today. In a similar vein, people are able to use their mobile phones anywhere in the world because there are universally accepted standards. The transmission of data through the air is accomplished

by wireless communication technology, which makes use of electromagnetic waves such as infrared, radiofrequency, satellite, and others. Figure 1.3 provides an illustration of some applications of wireless communication networks, including GPS, Wi-Fi, satellite television, wireless computer parts, wireless phones with 3G and 4G networks, and Bluetooth. These are just a few examples [6].

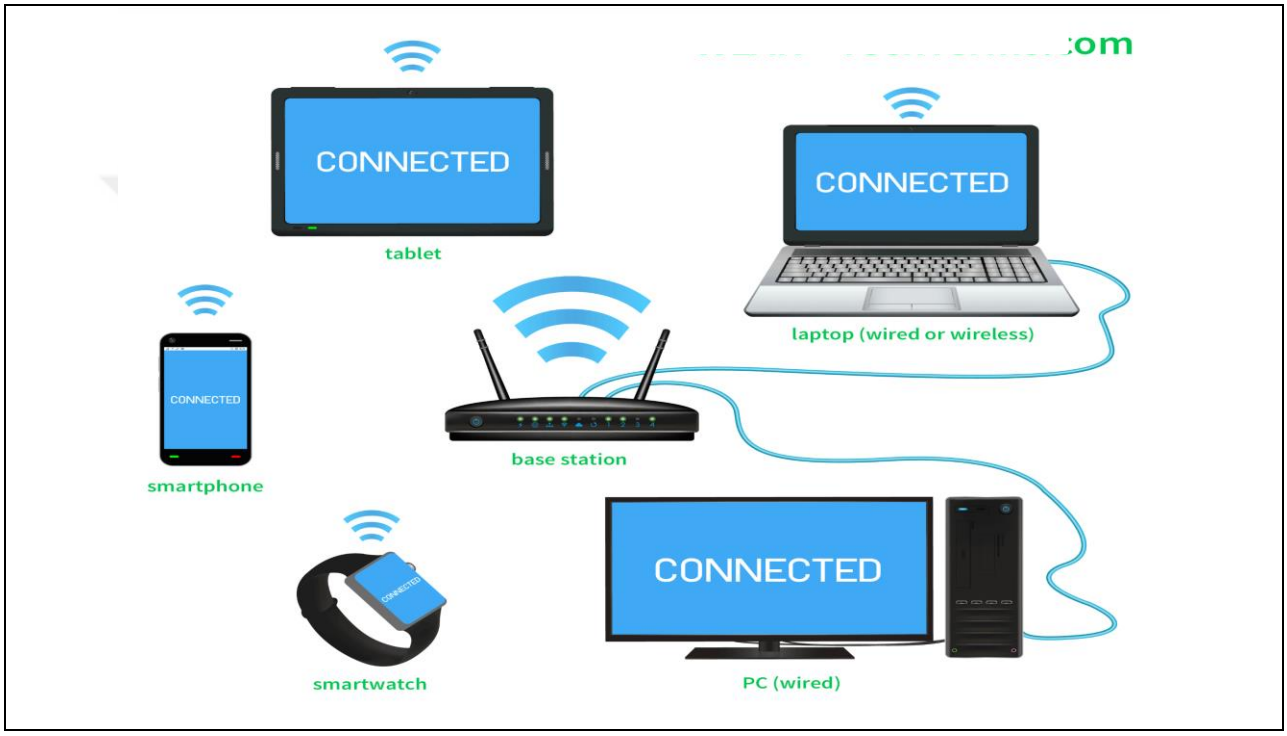

Figure 1.3: The Arrangement of Appliances in Small WLAN Network [6].

1.5 MILLIMETRE WAVES (MM-WAVES)

The communication systems via the mm-Waves were attracted a considerable attention when it comes to meeting future 5G network capacity requirements. The frequency ranges of the mm-Waves systems located in the range of 30 to 300 GHz with a total of around 250 GHz bandwidth, as illustrated in Figure 1.4. While the bandwidth range of mm-Waves frequencies is promising, but the propagation properties vary significantly in the term of the loss of the path among the transmitter and receiver, the diffraction and blocking that present in the path, the attenuation due to the rain such the fading effect, the absorbing of the signal by the atmospheric and foliage loss behaviour from microwave frequency bands. The total loss of the mm-Waves systems for point-to-point connections is generally significantly greater than that in the microwave systems.

Fortuitously, however, the mm-Waves frequencies characterised by the short wavelengths allow a great number of antenna elements to be extended in the same way, thus providing a high level of spatial treatment that is theoretically likely to recompense for the isotropic path loss at least. However, since mm-Waves systems are provided with various antennas, there are several difficulties in computing and implementing the expected performance gains of mm-Waves systems. For this purpose, the next sections of this chapter discuss key techniques for the link-level permitting of the 5G network based on mm-Waves. The connecting performance of the mm-Waves wireless system depends on a number of factors, e.g. whether we use beam-forming, multiplexing, or both, the method of channel identification, the way to structure the signal waveforms and access strategies [7].

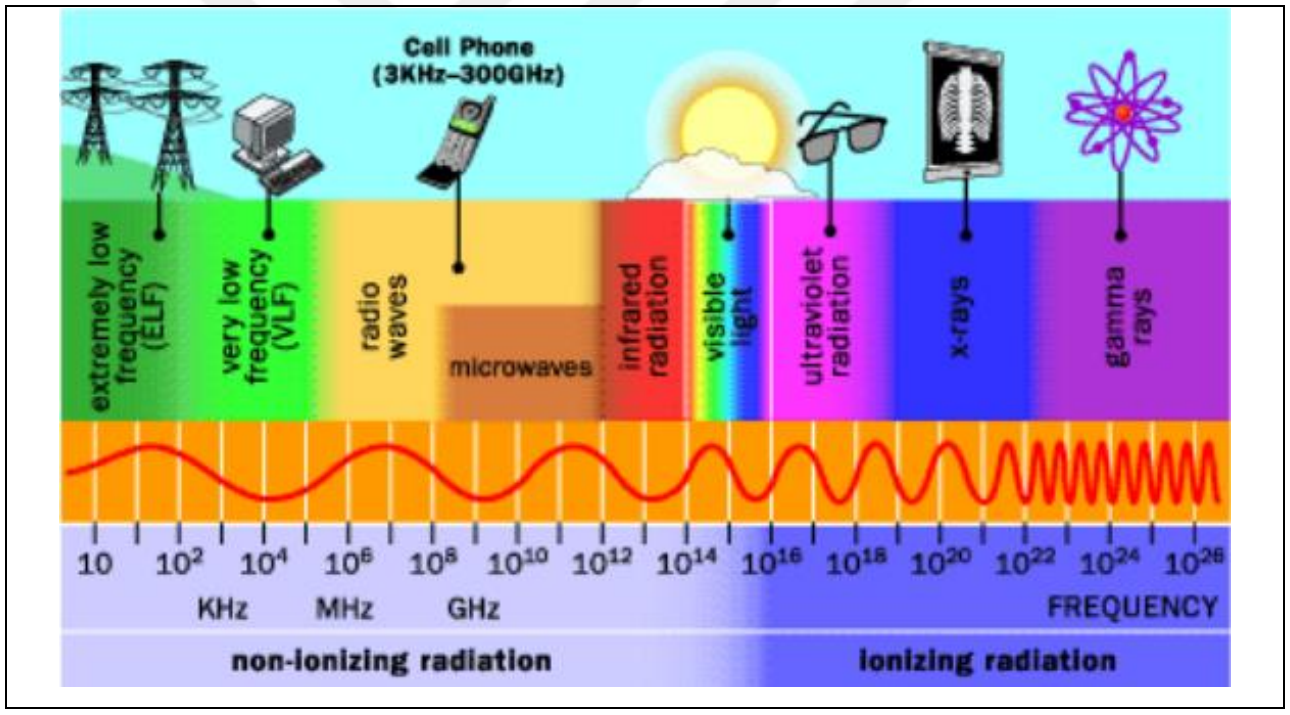

Figure 1.4: Electromagnetic Spectrum and its Applications [7].

1.6 PROPAGATION PROPERTIES OF MM-WAVES

In order to reach the 5G specifications, the spectral and energy efficiency of the applied right now 4th generation can be improved; the current network mainly overpopulated between 600 MHz and 3 GHz. The primary studies have however shown that the 5G network capacity alone cannot be achieved. For this reason, the mm-Wave frequency bands have attracted the researchers and the

network operators interest concerning to the meeting the capacity demands for the 5G network wherever there is a huge quantity of possible bandwidth in the mm-Waves. Although mm-Waves frequencies have a large bandwidth, the propagation features are quite different than those of the microwave frequency bands, which can be summarised in the next subsections [8].

1.6.1 Path Loss

According to Friis's law, the carrier frequency causes an increase in the isotropic path loss. A good illustration of this would be how the free-space path loss decreases as the square of the carrier frequency. When we locomote from 3 to 60 GHz as the carrier frequency, one can therefore anticipate experiencing consequential path loss in point-to-point communication [9].

1.6.2 Diffraction and Blockage

The diffraction lead to the propagation of the electromagnetic wave in a geometrical shadow zone in the end of the obstructions. The diffraction could lead to a non-negligible multi-path spread beneath the both of line-of-sight (LOS) and the non-line of-sight ($NLOS$) circumstances. According to the electromagnetic concepts, it is reasonably comprehended that electromagnetic waves face a problem to diffract during propagation within the obstructions which have a physical dimension much larger than its wavelength [10].

1.6.3 Rain Attenuation

The rain attenuation losses in the range of the mm-Waves frequency bands are usually extremely higher than those in microwave bands. The rain attenuation of about $10\ dB/km$ could be observed at a regular mm-Waves frequency of 73GHz, which is actually large [11].

1.6.4 Atmospheric Absorption

According to the field measurements, the mm-Waves signals are further liable to the oxygen reduction than the microwave signals. Around the 60GHz the mm-Waves signal, for example, there is a $20dB$ loss, Figure 1.4 illustrates the oxygen attenuation in the most frequencies of mm-Waves [12].

1.6.5 Foliage Loss

The foliage loss refers to the attenuation of radio signals caused by the appearance of trees that block the radio signal. Foliage losses for the mm-Waves are meaningful, and in some propagation environments, they can be a limiting factor. Empirical findings show that at 10m foliage penetration, the loss at the 80GHz mm-Waves frequency is nearby 23.5 dB, which is approximately 15 dB higher than the 3GHz microwave frequency [13].

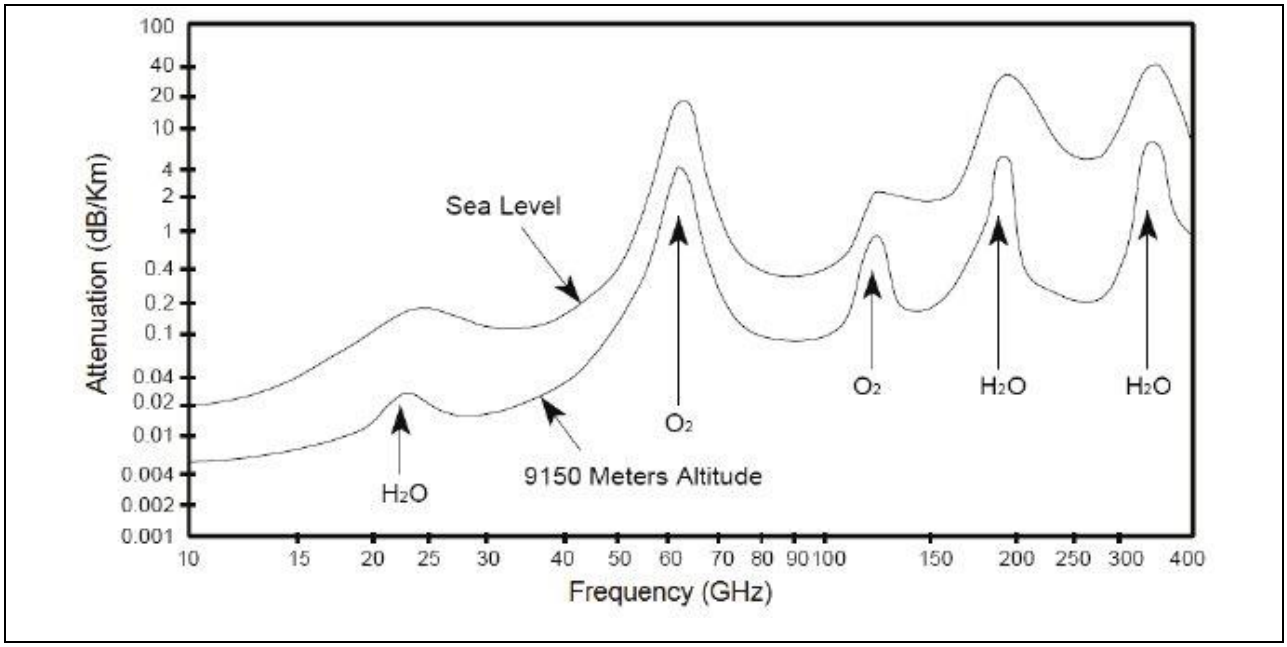

Figure 1.5: The Oxygen Attenuation Versus Frequency [13].

All of these pieces of evidence point to the conclusion that the mm-Waves systems have overall losses that are significantly higher than those of the microwave systems. Fortunately, the short wavelengths of the mm-Waves signals allow for a large number of antenna elements (i.e., antenna array) to be packed into a compact physical antenna area. This results in high spatial processing gains that can theoretically compensate for at most limited isotropic path loss. In other words, mm-Waves signals are able to compensate for at least some of the loss that is caused by isotropic path loss.

1.7 APPLICATIONS OF MM-WAVES

With the wide and rapid development in the field of communications and technology, there are many applications in which mm-Waves can be used to obtain good performance and data transfer speed, as illustrated in Figure 1.6. Some of these applications can be summarised as follows [14-16]:

a) **Fifth-generation and small cell theory:** the 5G is one of the very talked-about technologies in recent years. The mm-Waves will be practised in the 5G due to the requirement to backing the higher data rates (between 24-86GHz ranges). With the help of mm-Waves, tech companies are testing and investing in WLAN infrastructure. The mm-Waves could be utilised to implement the tiny cell idea in the future. The mm-Waves could be utilised to link mobile base stations alternatively to the conventional fibre optic transmission lines.

b) **High Definition (HD) video applications:** the ultra-high-definition video can be transmitted wirelessly to HD-TV utilising mm-Waves. Small transmission modules can be installed in the hardware of devices used for the transmission of high-definition video from digital set-top boxes, HD game stations, and other sources of high-definition video.

c) **WiGig Technology:** The WiGig is a technology developed by the "Wireless Gigabit Alliance" to promote the future of the audio and the video media things as well as wireless display interfaces at a gigabit speed. The WiGig transmission protocol allows for high-speed data transmission connecting appliances and computers.

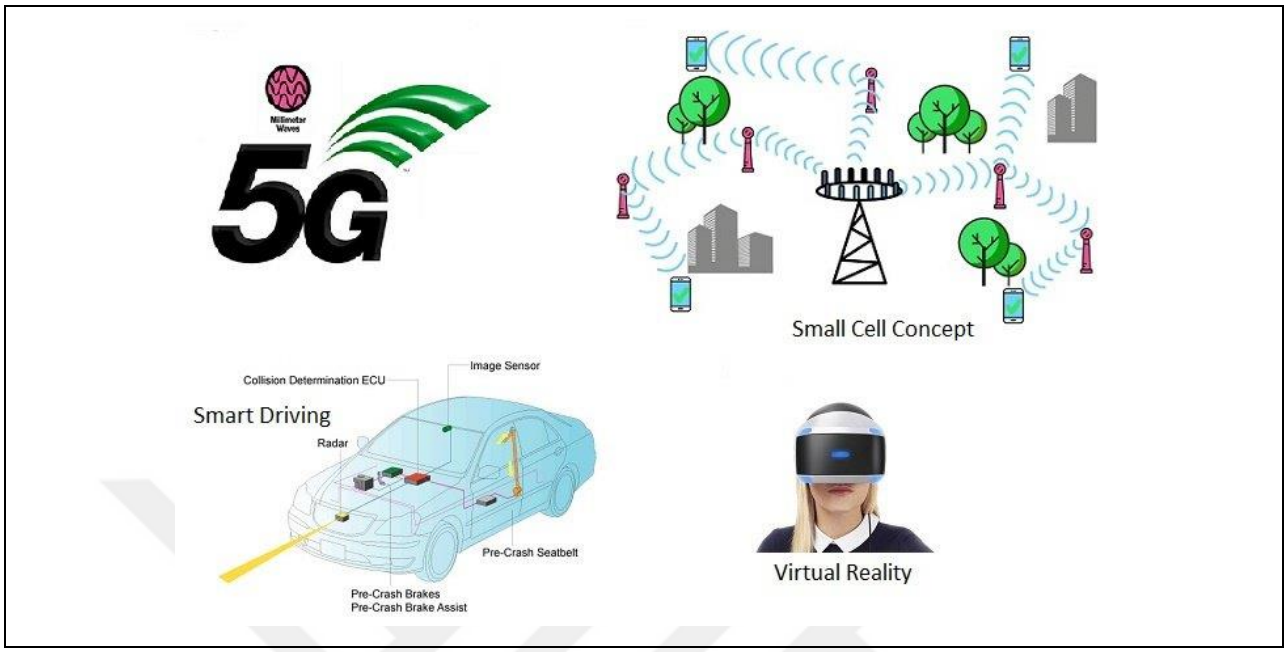

Figure 1.6: Some Applications of mm-Waves.

a) **Autonomous driving:** The concept of driverless cars is currently receiving a lot of attention in the field of technology. It is necessary to have detection of passengers and other obstructions in real time and with a low amount of lag time. It is essential to conduct accurate detection, and crucial choices must be made in a matter of milliseconds. mm-Waves are the most effective choice when looking for a radar that can detect automobiles.

b) **High-frequency radar:** The high-frequency radar technology has been growing and starting out for a variety of different employment opportunities. It does so by utilizing the beamwidth feature that mm-Waves provide. Using cutting-edge semiconductor technology, a miniature radar that fits on a single chip has been developed. This radar can detect and track a single target. Among the many applications are motion sensors, automatic doors, collision avoidance systems, intrusion alarm devices, and detection of vehicle speed.

1.8 LITERATURE SURVEY

Many studies, reviews, and investigations have been done previously regarding the design of fifth-generation antennas, some of which can be presented as follows:

a) In the previous work, a compact rectangular microstrip patch antenna (RMPA), triangular MPA, and triangular with slot MPA including a line feeding have been invented for the next-generation (i.e., 5G) communication systems at the license-free 60GHz frequency band. The designed RMPA was designed with a stout dielectric substrate with a small dielectric constant, which supports the wider bandwidth and better radiation. The RMPA performance was then tweaked for the best possible results. The simulated RMPA fitting for 60 GHz wireless applications for short-range high-speed communications (i.e., indoor applications), such as the transfer of audio and video data up to some Gb/s, due to its size, bandwidth, and gain [17].

b) In this work, the authors have been proposed a frequency reconfigurable RMPA for the THz application. The proposed RMPA comprise a slotted ground plane and the graphene material to realise the reconfigurability in the frequency. The proposed RMPA is enabled to be operated in several operation modes through varying the graphene material properties. This technique could substitute the ON and the OFF status of the traditional ways that utilised to construct the tunable antennas such as the PIN diode. During the operation in the diverse modes, the operating frequency band of the simulated RMPA varies in the range of 2.8-4.2THz. Proper radiation patterns, wide bandwidth larger than 10%, and an acceptable gain of 2dBi were reached throughout most of the antenna’s operation modes [18].

c) In this study, the researchers were introduced and studied an operating frequency band tunable RMPA with a circular substrate was designed utilising the metasurface (MS) structure to be operated around 5GHz. The MS is situated directly over the antenna radiated patch, presenting the proposed antenna extremely small size. The MS comprise rectangular-loop unit cells fixed regularly in perpendicular and straight directions. The obtained simulation results demonstrate that the proposed antenna's operating frequency band can be physically adjusted by rotating the MS about the center in relation to the patch antenna [19].

d) In this work, the authors have been designed and simulated a reconfigurable RMPA based on the PIN diode with probe feeding techniques for X-band applications. The proposed antenna comprises of square slot introduced at the outer of the rectangular patch as a frame to realise the PIN diode influence on the simulated antenna parameters. To make the tuning property on the proposed antenna the changing of the physical length is applied, this done be adding or removing the effect of the frame by the PIN diode through applied many values of the DC voltage on the diode. The structure of the proposed antenna has been simulated by utilising the ADS software [20].

e) The authors of this study presented a new approach to the voltage-controlled frequency reconfigurable RMPA (based on graphene material), which they introduced in their work. The simulated antenna is made up of a rectangular radiated patch and a microstrip stub that is attached at the end edge of the antenna radiated patch through the utilization of a graphene pad that is positioned between the ends of the antenna radiated patch and the stub. The proposed architecture makes use of the fact that the conductivity of graphene can be altered by the application of a bias voltage to the graphene layer. In the absence of any bias voltage, the graphene pad takes on the characteristics of an open circuit, in that it does not permit any current to pass through it and, as a result, the impact of the stub is nullified. After the dc voltage was increased, the graphene resistance decreased, which allowed current to flow through the sheet and into the stub. As a consequence, the patch antenna is capable of radiating at multiple frequencies. The RMPA under consideration was developed and evaluated at 5GHz. The researchers have been finally demonstrated that the frequency tunability can be increased by more than 10 percent despite the slight loss in gain [21].

1.9 PROBLEM STATEMENT

With the rapid and significant growth in the field of wireless communications, we have a major problem, which can be summarized by the large number of applications operating on the network, which causes congestion and interference that affects each other. In addition to users' ambitions to obtain high data transfer speeds of up to a few gigabits per second, it is suggested to switch to the next generation (i.e., 5G) of wireless communications. Where it is proposed to utilise the high frequencies in the mm-Wave band which is not utilised yet to obtain a large bandwidth that

contributes to the higher data rate. The big challenge in this range of frequencies is to design a small-sized antenna with good parameters, as the RMPA suffer from the narrow bandwidth and poor gain, so it is important to improve these parameters.

1.10 THESIS OBJECTIVES

The primary goal of this study is to create a frequency reconfigurable RMPA in form of a single element and array configuration for the 5G applications. Furthermore, the study's objectives can be summarised as follows:

Design, simulation, and optimisation of reconfigurable RMPA for 5G applications.

Utilise the graphene material as implanted slips within the rectangular patch of the proposed antenna.

Enhancing the proposed antenna gain by constructing a reconfigurable antenna array structure.

1.11 THESIS OUTLINE

This thesis comprises of four chapters, the outlines of each chapter can be summarised as following:

a) **Chapter Two:** This chapter covers the description of the fundamental parameters of the antennas, microstrip antennas, feeding techniques, array antenna, graphene material, and graphene material modelling.

b) **Chapter three:** This chapter illustrates the design procedure for the proposed reconfigurable RMPA by utilising the CST software. Additionally, this chapter presents the achieved results for the proposed reconfigurable RMPA such as S_{11}, BW, and antenna gain.

c) **Chapter three:** In this chapter we will present the conclusion that obtained from this study and also, we presents the future advices that could improve this work.

.

2. ANTENNA PARAMETERS AND GRAPHENE MATERIAL

2.1 INTRODUCTION

This chapter contains of many subsections which covers the antenna definition, antenna parameters, microstrip antennas, RMPA, feeding techniques, graphene material, and graphene material modelling.

2.2 ANTENNA DEFINITION

The antenna is a metal structure that is utilised to broadcast and collect electromagnetic energy from the free space (i.e., air). An antenna serves as a bridge between the guiding device (such as a waveguide or transmission line) and free space. The working principle of the antenna can be summarised by converting the electrical wave of the source into an electromagnetic radiated wave and vice versa. The antenna parameters, and various antenna characteristics, will be discussed in the following subsections [22].

2.3 FIELD REGIONS

The fields that are encirclement of the antenna can be subdivided into a three of the principal regions [22]:

a) **Far-field:** The far-field region is an extremely substantial region the reason for that because it utilised to determines the radiation pattern of the antenna. Ultimate of the antennas are operating in this range because they are utilised to communicate wirelessly over extended distances.

b) **Reactive near field:** In the immediate neighbourhood of the antenna is where you'll find the reactive near field. The fields in this zone are regularly reactive, which means that the E- and H- fields are out of phase with each other by ninety degrees (recall that fields that propagate or radiate are orthogonal (perpendicular) only when they are in phase).

c) **Radiating near field:** Radiating near field, also known as the Fresnel zone, is a region that is located between the near field and the far field. In this region, the reactive fields are no longer in control, and instead, the radiating fields are beginning to emerge. In contrast to the far-field

zone, the near-field zone exhibits significant variation in the form of the radiation pattern as one moves further away from the source.

2.4 ANTENNA PARAMETERS

In the next subsections, the necessary and fundamental parameters of the antenna will be briefly presented and discussed.

2.4.1 Radiation Pattern

The radiation pattern of an antenna is the graph that depicts the far-field radiation characteristic of the antenna as a function of the spatial coordinates that are designated by the elevation angle () and the azimuth angle () of the antenna. In other words, the radiation pattern can be described as the graph of the power radiated from the antenna per unit solid angle, which is the same thing as saying that the radiation intensity is all that there is to it. The antenna field regions were broken down and summarized in Figure 2.1 [22].

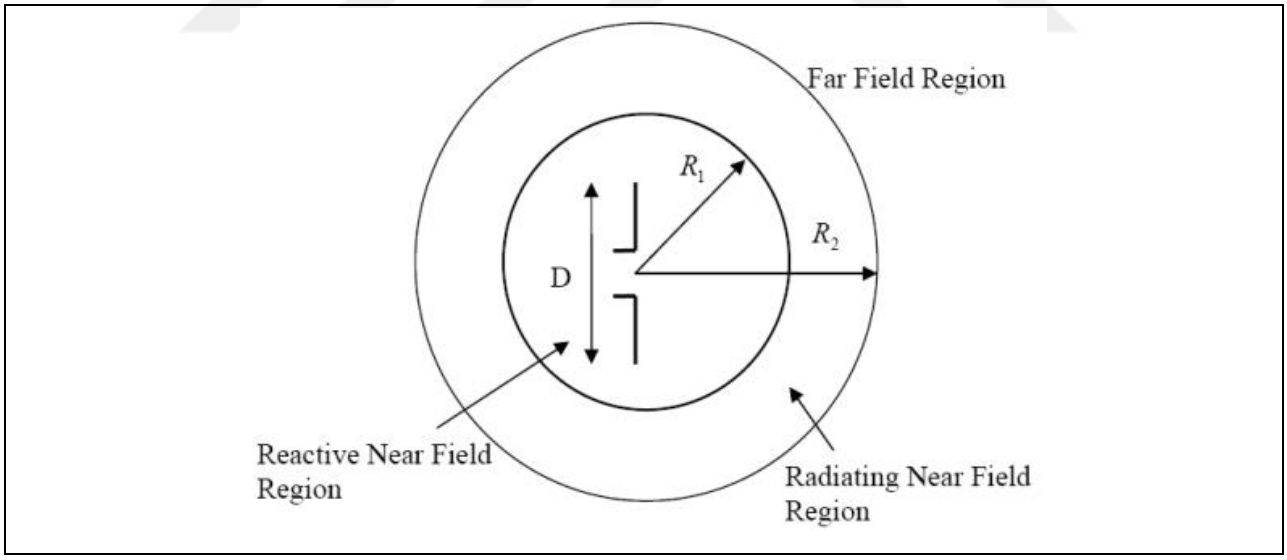

Figure 2.1: Antenna Field Regions [22].

Figure 2.2 shows the radiation pattern plot of a general directional antenna. The angle confronts by the half-power points of the major lobe is known as the half-power beamwidth. It is made up of two lobes: the major lobe and a minor lobe. The major lobe is the radiation lobe, which contains the greatest radiation way. The lobes that aren't part of the major lobes are called minor lobes. These lobes describe the radiation that is emitted in the undesirable directions.

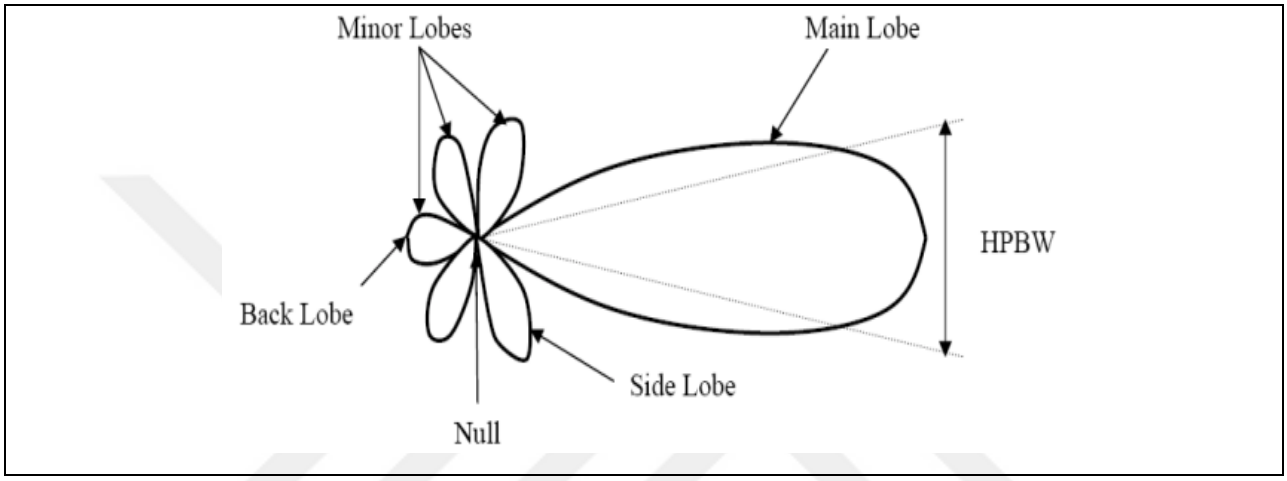

Figure 2.2: Antenna Radiation Pattern [22].

2.4.2 Antenna Directivity

The directivity of an antenna can be understood as the ratio of the antenna's radiation intensity in a single direction to the antenna's equalized radiation intensity in all directions. This ratio is referred to as the antenna's gain. In other words, the directivity of a non-isotropic source is determined by the ratio of the radiation intensity in a particular direction of a non-isotropic source to that of an isotropic source [22]. The antenna directivity (D) can be expressed in an equation form, as following:

$$D = \frac{4\pi U}{P} \qquad (2.1)$$

Where:

U : is refers to the radiation intensity of the antenna;

Ui : is refers to the radiation intensity of an isotropic source;

P : is refers to the overall power radiated.

Seldom, the direction of the directivity isn't designated, so that in such state, the direction of the highest radiation intensity is indicated and the highest value of the directivity given by expressed as follows:

$$D_{max} = \frac{4\pi U}{P} \qquad (2.2)$$

Where:

D_{max} : is referring to the maximum directivity;

U_{max} : is referring to the maximum radiation intensity.

Directivity, the ratio of two radiation intensities and can be considered as a dimensionless quantity. It is therefore usually described or measured in dB. The directivity of the antenna is a property that can be easily determined by analyzing the radiation pattern of the antenna. When compared to an antenna with a broad major lobe, one with a narrow major lobe would have greater directivity, making it the more directive option.

2.4.3 Antenna Impedance

The antenna's input impedance is defined as either the antenna impedance exhibited at its terminals or the voltage-to-current ratio at the terminal pair, the antenna impedance to be expressed as following:

$$Z_{in} = R_{in} + jX_{in} \qquad (2.3)$$

Where:

Z_{in}: is referred to the antenna impedance at the terminals;

R_{in}: is referred to the antenna resistance at the terminals;

X_{in}: is referred to the antenna reactance at the terminals.

The radiation resistance, denoted by R_r:, and the loss resistance, denoted by R_L, are the two components that make up the resistive part of the impedance, denoted by R_{in}. The resistive part of the impedance, denoted by R_{in}, is part of the input impedance. Figure 2.3 depicts the antenna equivalent circuit [23]. The power that is linked to the radiation resistance is the power that is actually radiated by the antenna, whereas the power that is consumed in the loss resistance is power that is spent as heat within the antenna itself. This is because of the nature of the material type that was used to manufacture the antenna, which was either dielectric or conducting losses.

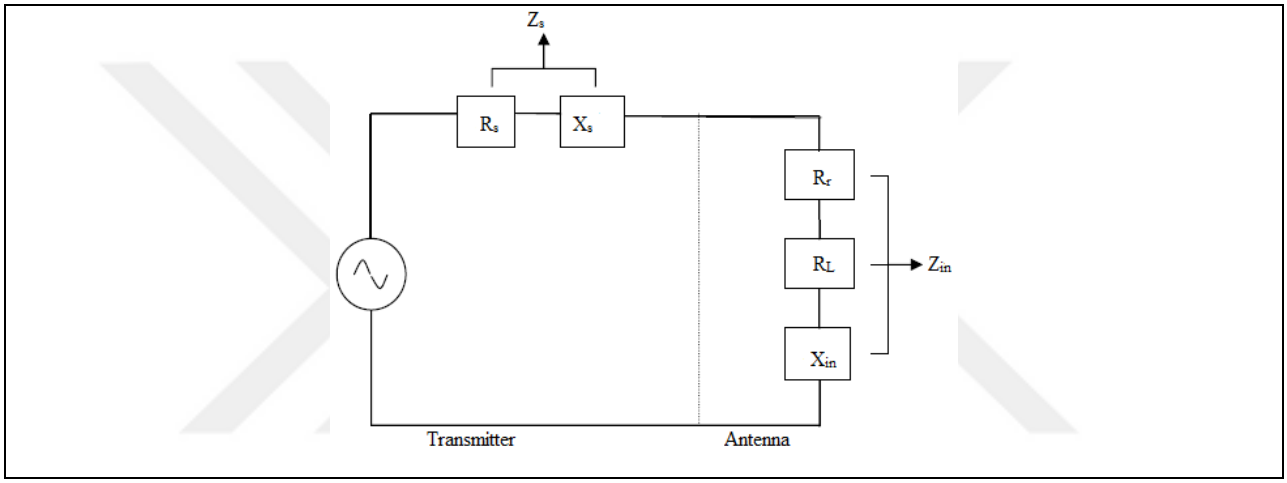

Figure 2.3: Antenna Equivalent Circuit [23].

2.4.4 Voltage Standing Wave Ratio (VSWR)

In order for the antenna to function in an effective manner, the maximum amount of power that can be transferred between the source of the electrical wave and the antenna must be accomplished. The maximum amount of power can be transferred between the source and antenna only when the impedance of the antenna (Z_{in}) exactly matches that of the source. According to the maximum power transfer theorem, the maximum amount of power can only be transmitted successfully under the following conditions: the impedance of the source must be a complex conjugate of the impedances of the antenna that is being considered, and vice versa.

$$Z_{in} = Z_s^* \qquad (2.4)$$

If the matching conditions are not met, somewhat the power may be reflected back toward the source, this which leading to standing waves that may be characterised by a parameter called the VSWR. The VSWR can be expressed in the equation form as following:

$$VSWR = \frac{1 + |\Gamma|}{1 - |\Gamma|} \qquad (2.4)$$

$$\Gamma = \frac{V_r}{V_i} = \frac{Z_a - Z_S}{Z_a + Z_S} \qquad (2.5)$$

Where:

Γ: is referred to the coefficient of the reflection;

V_r: is referred to the amplitude for the reflected wave;

V_i: is referred to the amplitude for the incident wave.

The VSWR is a measurement of the difference in the impedance among the source and the antenna. The greater value of VSWR means that there is a higher mismatch. The best matching occurs when the unity VSWR reached, for the most of systems design the input impedance is about 50 or 75Ω [23].

2.4.5 Return Loss (RL)

The antenna RL is the most meaningful parameter that is useful when analysing the performance of the antenna. This parameter is linked with the impedance matching and the maximum power transfer theory. The RL represents the efficiency of the power transmission from the source of the power to the antenna. The RL is represented by the proportion of the input power to the antenna ($P\ (in)$) to the power that returned or reflected back from the antenna terminals toward the source direction ($Pref$). Once this ratio of ($P(in\ )/Pref\ $) raised, this is the preferable case and implies that the arrived and received power by the antenna is greater than that reflected to the source, the RL of the antenna can be represented as following [23]:

$$RL = 10log\left(\frac{P\ (in)}{Pref}\right) \quad (dB) \qquad (2.6)$$

2.4.6 Antenna Bandwidth (BW)

The bandwidth (BW) of the antenna can be thought of as the range of frequencies that are in use during the time period in which the performance of the antenna satisfies a particular requirement regarding some aspect of its makeup. The input impedance, radiation pattern, beamwidth, and gain of an antenna are all compared to their values at the center frequency to determine the bandwidth. The frequency ambit on each side of the center frequency (i.e., right and left) is referred to as the frequency ambit on each side of the center frequency. The broadband antenna, abbreviated as BW, can be conceptualized as the ratio of the upper to the lower frequencies that are acceptable. Practically, the antenna BW can be obtained and determined from the antenna RL at the RL=-10 dB, a horizontal line is applied to determine the f_L and f_H then the BW will be the difference between the two frequencies [24], as illustrated in Figure 2.4.

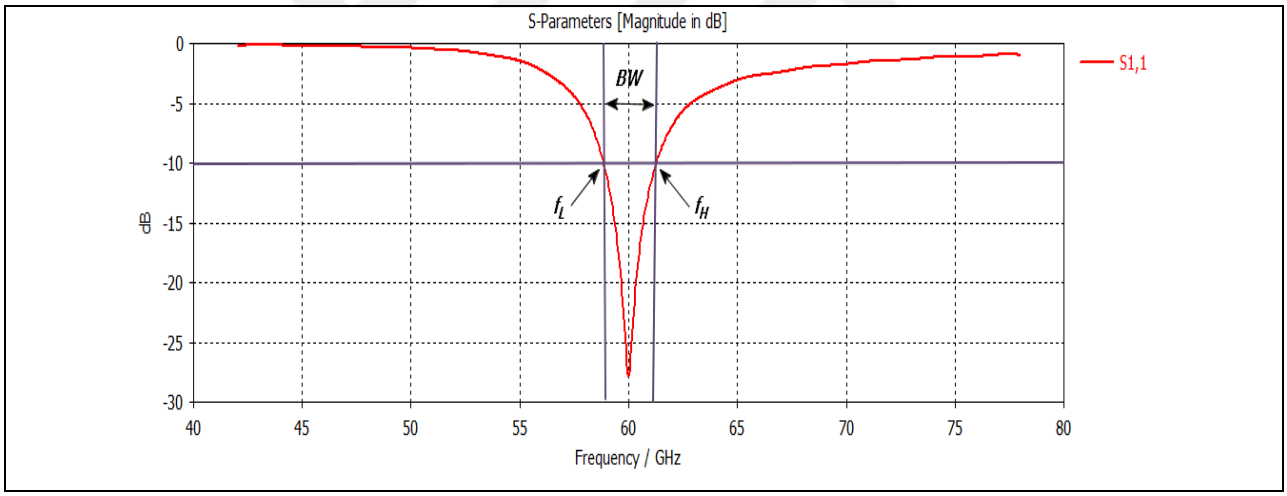

Figure 2.4: Calculation of BW from RL plot.

2.4.7 Antenna Efficiency

When analyzing antenna performance, one of the most important parameters to take into consideration is the antenna's efficiency. The efficiency of the antenna takes into account not only the number of losses that are available at the terminals of the antenna but also losses that are present within the structure of the antenna; these losses are outlined in the following manner [22]:

a) Reflections due to the mismatch among the source and the antenna

b) I^2R losses which are conduction and dielectric losses.

In the mathematical form the efficiency of the antenna (e) can be expressed as follows:

$$et = er\ ec\ ed \tag{2.7}$$

Where:

et: is referring to the total antenna efficiency;

er: is referring to the reflection (mismatch) efficiency;

ec: is referring to the conduction efficiency;

ed: is referring to the dielectric efficiency.

Because the e_c and e_d are hard to separated, they are lumped together to form the e_{cd} efficiency which is given as:

$$e_{cd} = ec\ ed = \frac{Rr}{Rr + Rl} \tag{2.8}$$

Where:

e_{cd}: is referring to the efficiency of the antenna.

2.4.8 Antenna Gain

The gain of the antenna is another essential parameter that is inextricably linked to an antenna's degree of directional behavior. The directivity of the antenna has already been discussed; this quality describes the degree to which an antenna concentrates energy in one direction in comparison to the energy concentrated in the other directions. As a consequence of this, if the antenna is 100 percent efficient, the directivity of the antenna and the gain of the antenna will be comparable, which will result in the antenna functioning as an isotropic radiator. The gain is the result of power being gained in one direction at the expense of power being lost in the other directions. This is due to the fact that all antennas radiate more in one direction than in the other directions. A constant association exists between the gain and the major lobe, and it is always denoted in the direction of maximum radiation, unless something different is specified. [23].

2.5 MICROSTRIP ANTENNAS (MAS)

The MAs are a comparatively new technology. It was created to make it easier to integrate an antenna and other communication system driving circuitry on a single printed circuit board or semiconductor chip. Aside from the other benefits, the antenna fabrication using integrated-circuit technology permitted for the high dimensional precision, which was otherwise challenging to produce using traditional fabrication means. The MAs geometry is made up of a dielectric material usually named as substrate with a thickness of "d", complete metallization on the face, and a metal named as the "patch" on the bottom. Typically, the substrate is thin and selected to be about ($d \ll \lambda$). Although a rectangular shape, as shown in Figure 2.5, is usually utilised, the metal patch on the face of the dielectric material can take on a variety of geometries, Figure 2.6 illustrates many of the geometries that can be utilised for the designing of the patch. Numerous approaches can be used to excite (i.e., power feeding) the antenna. One popular approach is to feed the MA on a microstrip line by attaching the line to one of its edges. The microstrip line can be directly supplied through attaching a signal source across the microstrip line and the ground plane, or it can be joined to a feeding circuitry [22].

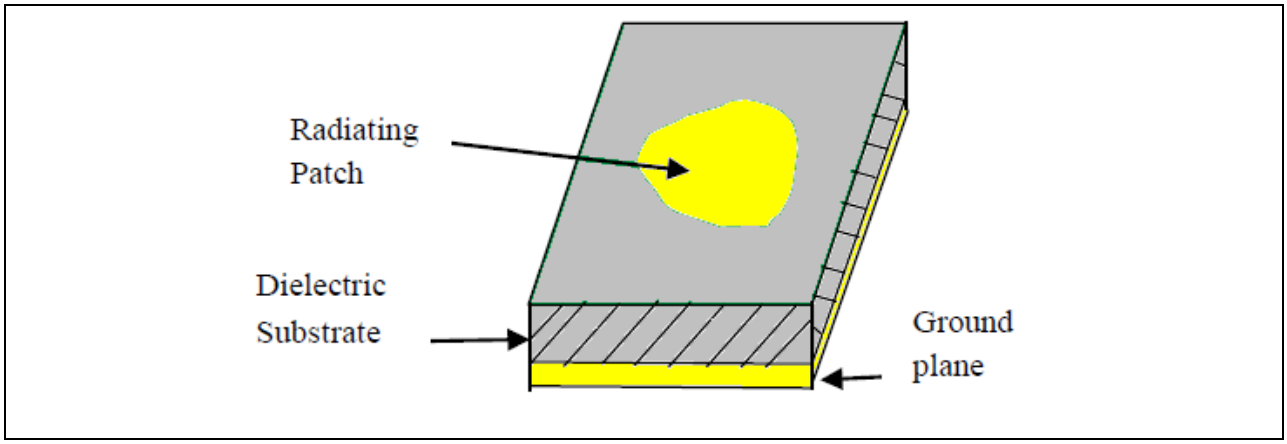

Figure 2.5: Geometry of the MA.

The broadside (vertical on the substrate) of the microstrip antenna produces the most radiation, while the end-fire (onward the substrate's surface) produces the least. The antenna's dimensions ordinarily chosen so that it resonates at the operating frequency, resulting in a real input impedance. This necessitates a rectangular MA beside a length (L) of approximately half a wavelength in the dielectric medium. The value of the input impedance is controlled by the width

of the antenna, which is denoted by W. The MA appears to have the shape of a rectangular cavity that is adjacent to an open sidewall. The fringing fields that travel through the open sidewalls are what ultimately cause the radiation to be emitted. However, the structure is primarily composed of resonant cavities, with only a trace amount of fringing radiation. As a direct consequence of this, the bandwidth of the radiation is poor.

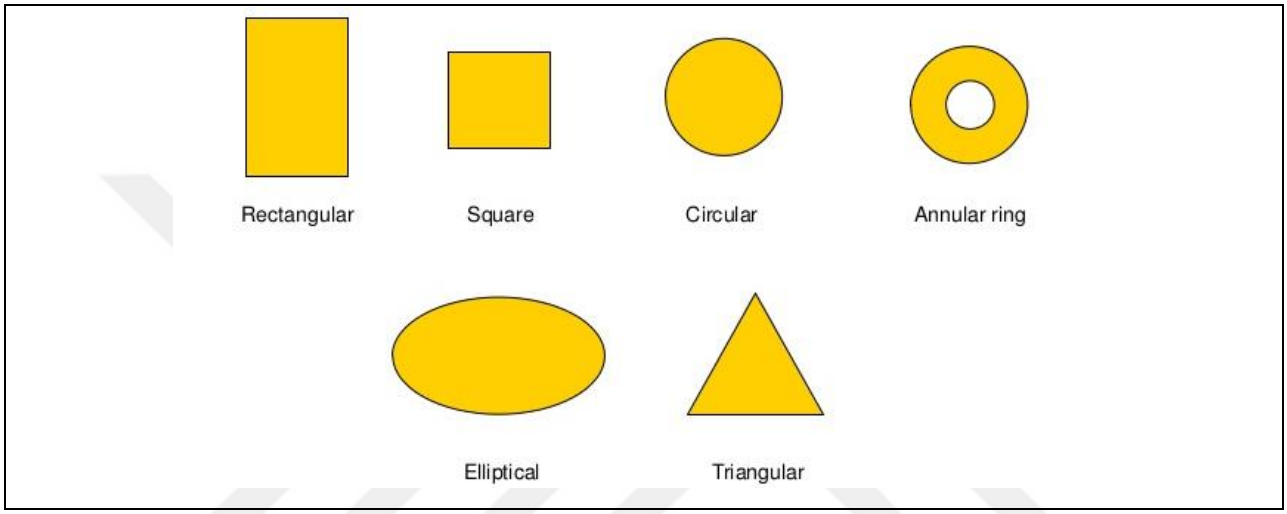

Figure 2.6: Common patch shapes [22].

2.6 RECTANGULAR MPA

The RMPA that resembles a pruned microstrip transmission line is the extremely utilised antenna. Its dimensions measured to be about half a wavelength in length. In the event that air is utilized as the dielectric substrate, the RMPA is approximately equivalent to one-half of the wavelength of free space. When an antenna is loaded with a dielectric as its substrate, the length of the antenna is minimized so that it has the greatest possible effect on the relative dielectric constant of the substrate. Figure 2.7 depicts the configuration of the RMPA, which is necessary because of the extension of the electric "fringing fields." These fields cause the electrical length of the antenna to be slightly longer than its physical length [23].

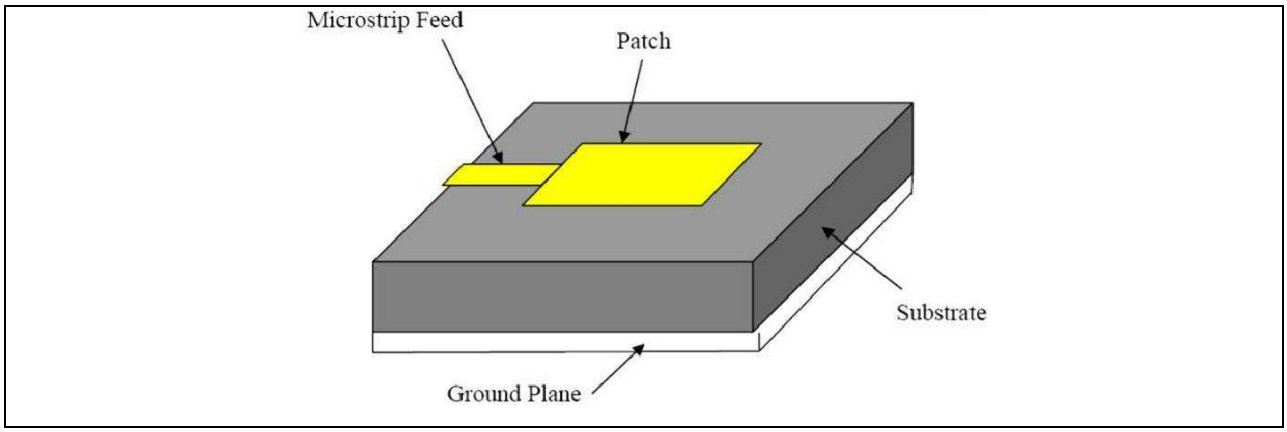

Figure 2.7: Configuration of the RMPA [23].

2.7 FEEDING TECHNIQUES

In order, to powering the RMPA there are several approaches can be utilised. The most popular approaches can be divided into four categories as follows [25]:

a) **Microstrip line:** In this approach of the feed technique, a direct conductive stripline is coupled directly to the one edge of the radiating patch, as presented in Figure 2.7. The width of this stripline is significantly narrower than the width of the radiating patch. This particular kind of feeding approaches can be engraved over the antenna substrate so that they are on the same face as the patch, which results in a structure that is planar. An inset cut could be incorporated into the patch rather than any additional matching component being used in order to achieve a better coupling between the patch and the feed line. This would be done in order to achieve the desired result. This is achieved by exercising appropriate control over the position of the inset.

b) **Coaxial probe:** The coaxial feed, which is also known as the probe feed, is recognized as being one of the most traditional methods for feeding the RMPA. Figure 2.8 demonstrates that the inner conductor of the coaxial connector travels through the dielectric and is soldered to the patch, while the ground plane of the antenna is connected to the outer conductor of the connector.

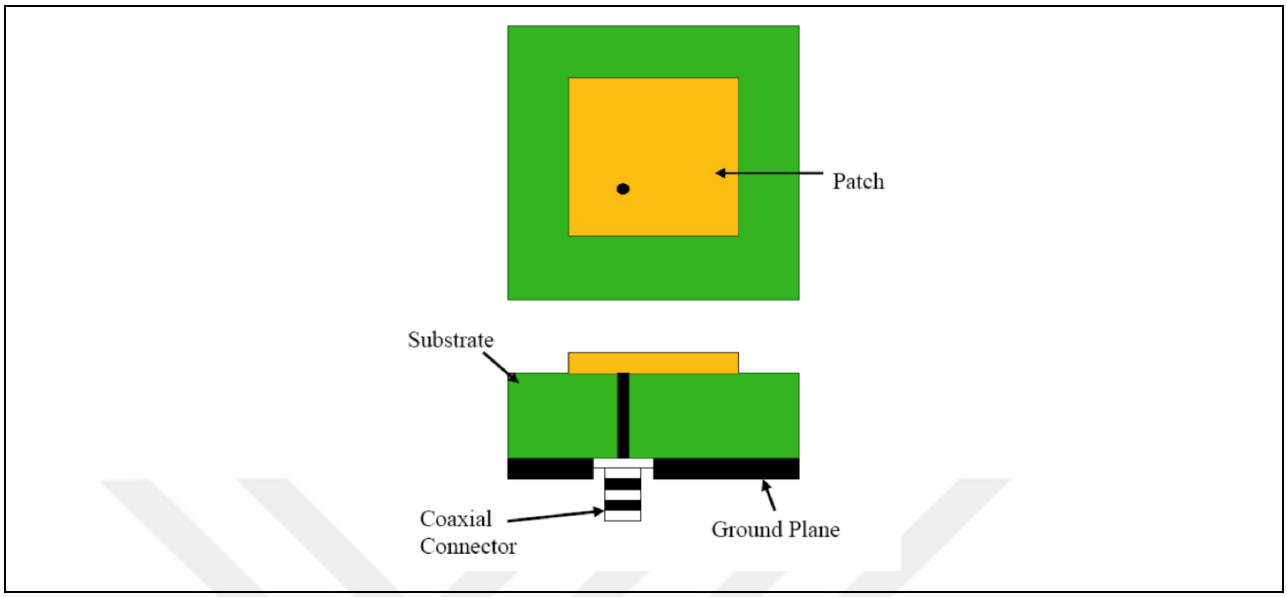

Figure 2.8: Coaxial feed scheme [25].

The primary advantage of this strategy for feeding can be summed up by the selection of the position of the feed point, which allows the feed to be fixed at any location within the patch to achieve impedance matching among the patch, the port, and the signal. This method of feeding produces a low amount of dummy radiation, and it is not difficult to construct. The most significant drawback associated with it is that it possesses a narrow bandwidth, and it is challenging to model because it requires a hole to be pierced into the substrate. In addition, for substrates that are thicker, a longer probe length causes the input impedance to become more inductive, which results in issues with matching.

c) **Aperture coupling:** As shown in Figure 2.9, the aperture coupling is accomplished by etching the radiating microstrip patch element that is located on the top of the antenna substrate and the microstrip feed line that is located on the bottom of the feed substrate. This creates a gap between the two that allows for the transmission of electromagnetic waves. As a consequence of this, the thickness and dielectric constants of these two substrates were able to be calculated on an individual basis so that the various electrical functions, including circuitry and radiation, could be optimized. As a consequence of the symmetry of the configuration, the coupling aperture is typically centered beneath the patch. This results in cross-polarization that is significantly reduced.

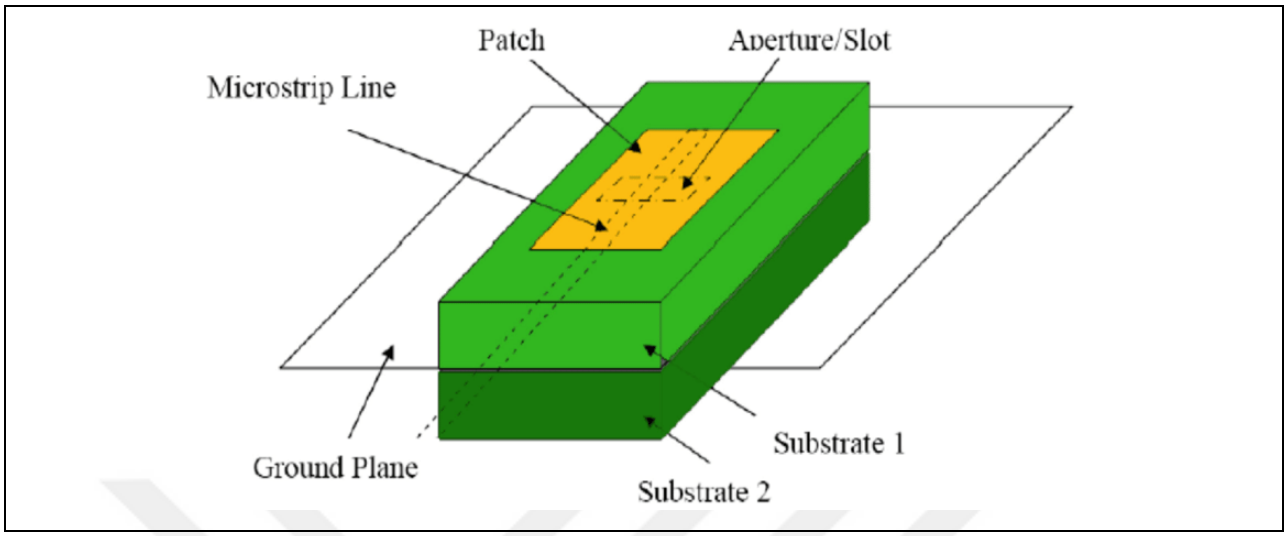

Figure 2.9: Aperture couple feeding [25].

The magnitude of the coupling that occurs between the feed line and the patch is determined, in part, by the aperture's dimensions, shape, and placement. The patch and the feed line are physically separated by the ground plane, which helps to reduce the amount of spurious radiation. Therefore, there is symmetry in the configuration.

d) **Proximity coupling:** This method of feeding also goes by the name electromagnetic coupling approach, which is just another name for it. In this method, two dielectric substrates are utilized, as shown in Figure 2.10, with the feed line between the two substrates and the radiating patch on top of the upper substrate. Additionally, the patch that emits radiation is placed on top of the upper substrate. Because the overall thickness of the RMPA is increased, the primary advantage of this feed approach is that it rejects the spurious feed radiation and provides a very high bandwidth of approximately 13 percent. This is made possible by the increase in the overall thickness of the RMPA. This method also enables the selection of two distinct dielectric media, one of which can be used for the patch and the other for the feed line, in order to optimize the performance of each component individually.

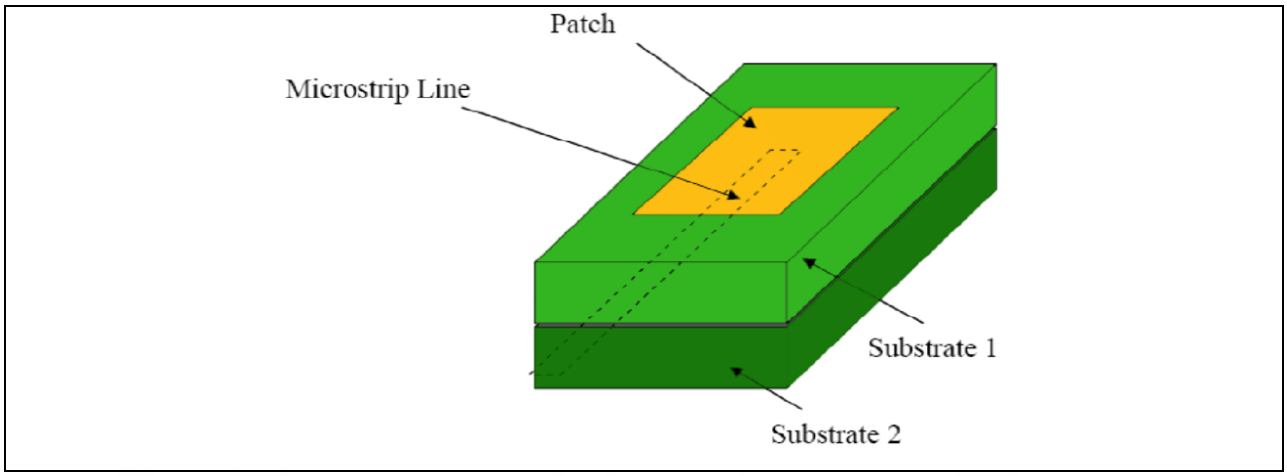

Figure 2.10: Proximity coupled feeding [25].

The most significant drawback of this feed scheme is that it is difficult to fabricate. This is primarily caused by the presence of two dielectric sheets, each of which needs to be aligned in the correct manner. In addition to this, the overall thickness of the antenna has become significantly thicker. The rapid development of wireless communications holds the promise of making interactive voice, data, and video services available whenever they are needed and from wherever they may be accessed. Small handheld devices all the way up to wireless local area networks are included in the broad category of wireless communication systems that can be purchased today.

2.8 RECTANGULAR MICROSTRIP PATCH ANTENNA (RMPAA) CONFIGURATION

The RMPAA is a configuration utilised to enhance the antenna parameters. The antenna array is produced from a group of RMPA elements that all have the same or equivalent characteristic. When compared to a single RMPA, the "grouping" of antennas (i.e. array configuration) increases the gain. At the same time, the power that is radiated is directed more intently in a single direction. This is because single-element antennas have a more limited beamwidth than their multi-element counterparts. Radiation properties of an antenna array are determined by the detachment distance between individual antenna elements as well as the orientation of those elements. The variation in phase and amplitude that occurs among the antenna elements is another factor that governs the radiation pattern and gain of the antenna array. The electronic control of these phase and amplitude variations makes it possible to exercise control over the beamforming process. This demonstrates that it is possible for the radiated power to be aimed in the direction of the receiver. Electronic control of phase and amplitude differences makes it possible to effectively pursue a moving target.

This is made possible thanks to the advancement of technology. The utilization of an antenna system such as this one for a man-machine link is predicated on this overarching idea. Figure 2.11 illustrates the structure of 4×1 RMPAA [26].

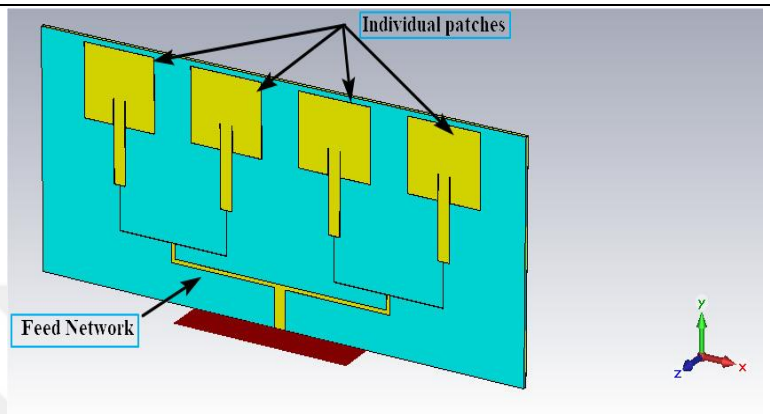

Figure 2.11: Structure of 4×1 RMPAA

2.9 GRAPHENE MATERIAL

Graphene material is made from the carbon atoms arranged to be in the form of hexagonally positioned, as illustrated in Figure 2. Such organisation makes the graphene in a single atom stout.

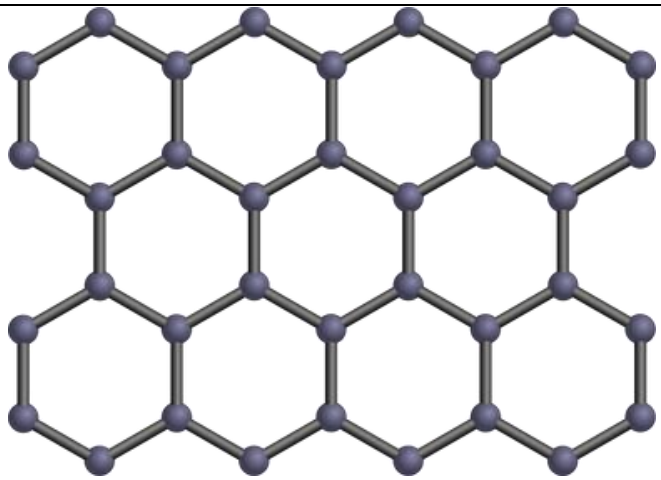

Figure 2.12: Graphene material structure [27].

Graphite, which is one of the substances that can be found in the greatest quantities on our planet, is the component that makes up this material (graphite can be found, for example, in the mines of our pencils). One millimetre of the graphite material can be broken down into three million layers of graphene [27].

2.9.1 Graphene Material Characteristics

Graphene is a material that possesses a number of fascinating properties. Graphene is a material that has been the subject of extensive research and has a diverse range of potential applications as a result of its properties, which include the abundance of carbon in the earth's crust and the ability to produce it easily. The following are some of graphene's most notable characteristics [28]:

a) Large thermal conductivity

b) Large electrical conductivity

c) Great flexibility

d) High rigidity

e) A strong material, where Graphene is roughly 200 times stronger than steel material, similar to diamond resistance, but extremely greater.

f) Ionising radiation is not affected

g) Capable to produce electricity by exposure to sunlight

h) limpid material

i) In comparison to other compounds, the Graphene consumes less electricity.

2.9.2 Graphene Applications

Because of its outstanding characteristics, the graphene material has applications in a wide range of fields, the most well-known of which are depicted in Figure 2.13.

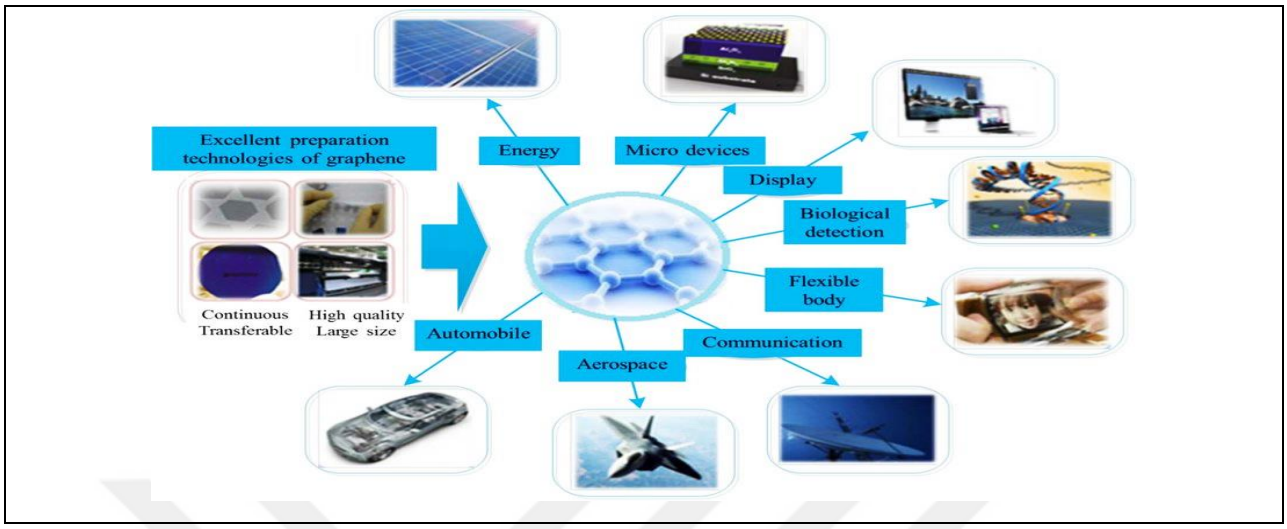

Figure 2.13: Some of graphene material applications [28].

In the field of electronics, graphene is utilized in the manufacturing of microchips and transistors, as well as the development of conductive inks that make it possible to print electronic circuits. Graphene has the potential to significantly enhance the efficiency with which renewable energy sources, such as solar energy, are utilized. By incorporating this material into solar panels, it is reasonable to expect an increase in their efficiency as well as an increase in the amount of energy they produce. By increasing battery autonomy and reducing charging times, the use of graphene in batteries in the automotive industry will enhance the performance of electric vehicles. Graphene is a two-dimensional carbon material.The other graphene material applications can be summarised as following [29]:

a) **Security labels:** The safety labels were the first and probably the first effective and real application of graphene.

b) **Padel blades:** Now there are products in the sports production that include graphene in their organisation. Paddle blades are an example of this, where graphene can be utilised on the faces of the blades, on the impression surface, or on the frame to increase their resistance and duration.

c) **Medical sensors:** Another of graphene's characteristics is its capability to detect very little amounts of the substances. Graphene has the ability to identify a single molecule in a large volume. Graphene oxide has been used to improve these characteristics, and some medical

companies are already selling sensors based on graphene. Graphene has a number of potential applications in the medical field.

d) **Military Applications of Graphene:** Nanotechnology is beginning to be used for the benefit of the arms industry, in addition to its many other applications. This opens the door to the development of new weapons that are both extremely effective and devastating. Rifles of all types can now be produced thanks to graphene and nanotechnology. Integrated computers would enable remote control of any weapon, as well as a more compact assisted operation, which would improve robotics. Furthermore, because these materials would be made with a minimal amount of metal, radar detection would be much more complex.

2.9.3 Graphene Modelling

In the field of communications and electronics, when dealing with graphene, the most important parameter is the conductivity of electric current, through which we can find the surface impedance of graphene. The graphene is characterised by one of the special and unique properties that no other material possesses in nature, which can be summarised by its variable and tunable surface conductivity. The surface conductivity changes when a DC voltage is applied to the graphene sheet. Once the applied DC voltage is raised, the density of the charge carrier risen in turn, following a rise in the graphene conductivity and which meaning minimising the graphene surface impedance. The graphene conductivity is separated into two fundamental parts: are the intra-band, which dominates in the total conductivity in the frequency range under 5 THz, and the inter-band, which has no consequence on total surface conductivity in this band and could be overlooked; nevertheless, its impact will fall apparent once the frequency range is exceeded the mentioned frequency, Figure 2.14 illustrates the graphene material conductivity against the frequency [30].

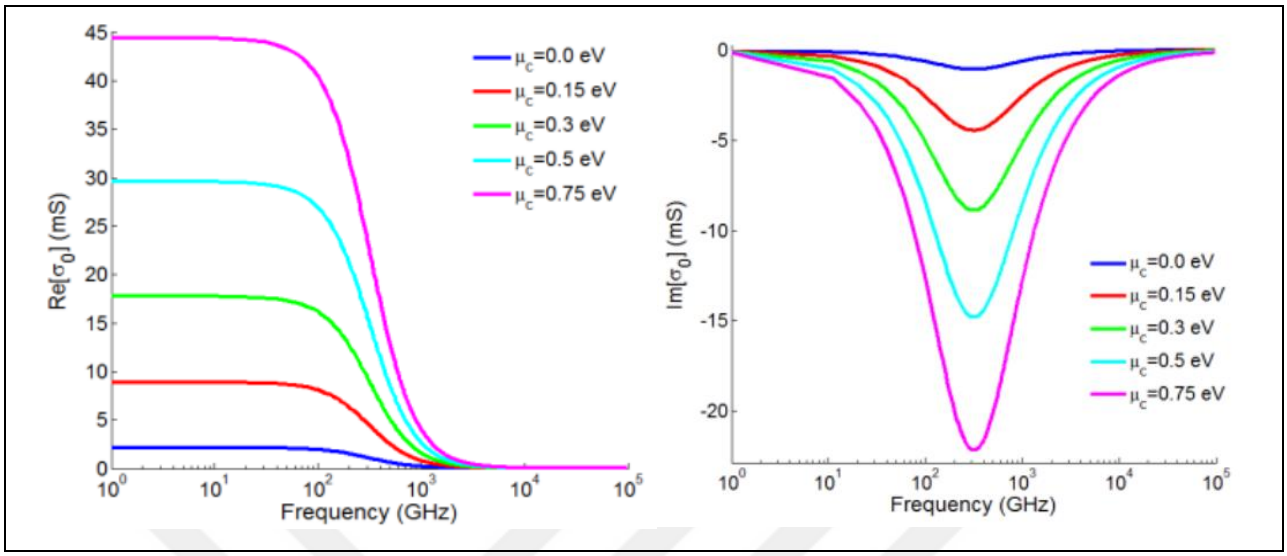

(a) Real part. (b) Imaginary part.

Figure 2.14: Graphene surface conductivity against frequency [30].

In order to model the graphene conductivity a special mathematical equation can be utilised, which summarised as follows [30], [31]:

$$\sigma_{AC} = \frac{-jq^2 k_B T}{\pi\hbar^2(\omega - j\tau_t{}^{-1})}\left(\frac{\mu_c}{k_B T} + 2ln\left(e^{-\frac{\mu_c}{k_B T}} + 1\right)\right) \quad (2.9)$$

Where:

σ_{AC}: Is referred to the graphene alternating current conductivity;

ω: Is referred to the angular frequency;

μ_c: Is referred to the chemical potential;

τ_t: Is referred to the relaxation time;

T: Is referred to the room temperature;

q: Is referred to the elementary charge;

$\hbar$ Is referred to the reduced Planck's constant;

k_B: Is referred to the Boltzmann constant.

The chemical potential of graphene material is associated with the carrier density n $(1/m^2)$ that could be determined from the following equation:

$$\mu c = \hbar v_{fer}\sqrt{n\pi}, \qquad (2.10)$$

Where:

v_{fer} = Is referred to the Fermi velocity of graphene and equal 1×10^6 (m/s).

The value of n can be sequentially tuned by subjecting a DC voltage on the graphene sheet which can be obtained from the following equation:

$$n = \frac{\in_o \in_r \ V_a}{dq} \qquad (2.11)$$

Where:

$\in_o$: Is referred to the free space (air) permittivity (F/m);

$\in_r$: Is referred to the relative dielectric constant;

V_a: Is referred to the DC voltage;

d: Is referred to the graphene layer thickness;

q: Is referred to the electron charge.

The graphene surface impedance can be determined from the graphene conductivity equation (2.9) as follows:

$$Z_s = 1/\sigma_{AC} \qquad (2.12)$$

$$Z_s = \frac{j\pi\hbar^2(2\pi f(\tau_l\tau_s) - j(\tau_l+\tau_s))}{q^2(\tau_l\tau_s)\left[\mu_c + 2k_BTln\left(e^{-\frac{\mu_c}{k_BT}}+1\right)\right]} \qquad (2.13)$$

The scattering effects τ_l can be determined as following:

$$\tau_l = \frac{\mu_l \hbar\sqrt{n\pi}}{q\, v_f} \tag{2.14}$$

Where:

μ_l: Is referred to the mobility electron.

The value of τ_s is can be determined as following:

$$\tau_s = \frac{4\hbar^2\, \rho_m {v_{ph}}^2 v_f}{\sqrt{n\pi} k_B T\, D^2} \tag{2.15}$$

Where:

ρ_m: Is referred to the 2D mass density of graphene and equal 7.6×10^{-7} (Kg/m^2);

v_{ph}: Is referred to the sound velocity of longitudinal acoustic phonons in graphene and equal 2.1×10^4 (m/s);

D: Is referred to the deformation potential (eV). However, in some previous studies its values around ~18 eV appears to be a prevalent and recognised value for graphene on a dielectric substrate.

3. ANTENNA DESIGN AND SIMULATION

3.1 INTRODUCTION

This chapter presents the necessary preliminary steps for designing the proposed antenna using graphene material. It also provides an explanation and discussion of the results that we obtained from the simulation program after the design and run process is completed.

3.2 ANTENNA DESIGN

In order to design any antenna, three basic things should be taken into account, which can be said that they are:

a) Resonant frequency (f_o)

b) The dielectric constant value (εr)

c) The height of the dielectric (t), which are set as presented in Table 3.1.

Table 3.1: The Selected Antenna Parameters.

Parameter	Value
f_o	29GHz
εr	2.2
t	0.1mm

The proposed design for the reconfigurable RMPA/RMPAA is giving a satisfactory reconfigurability ambit to recompense the narrow BW that is one of the disadvantages of the MPA. In accordance with some of the previous studies, the mm-Waves antenna that made totally from the graphene material are predicted to have poor performance and very modest reconfigurability ambits. So that it is suggested to utilise a hybrid of the copper material and some flakes of graphene implanted within the antenna patch to obtain acceptable performance. To design the proposed reconfigurable MPA/MPAA for the 5G applications, the shown steps in Figure 3.1 is utilised.

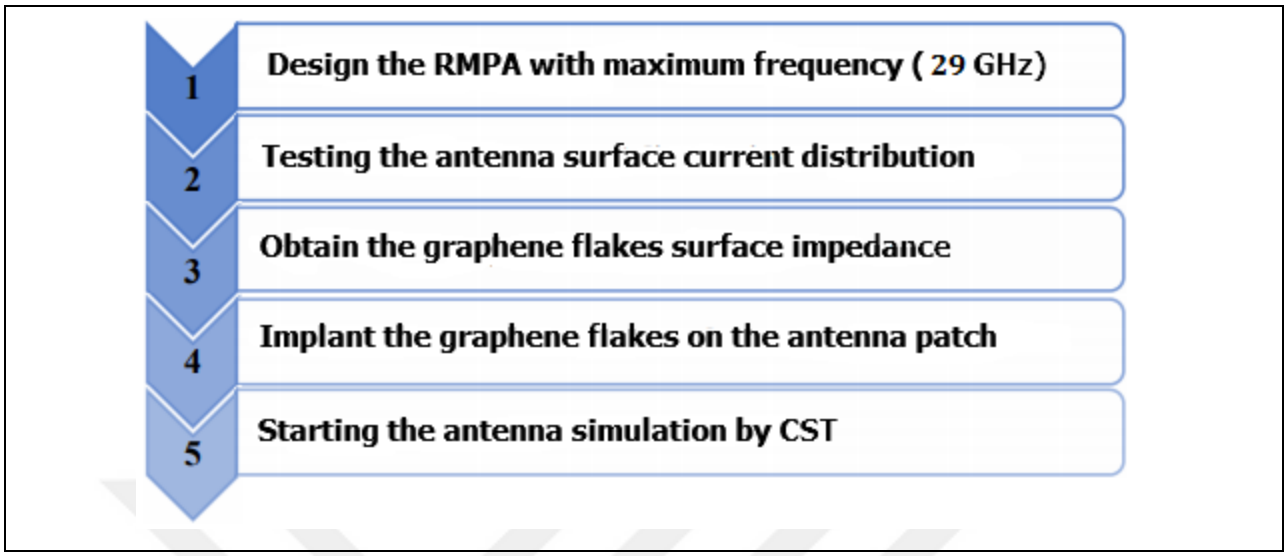

Figure 3.1: Steps of Reconfigurable RMPA Design.

3.2.1. RMPA Design

In this part, the simulation process of the traditional RMPA is designed and simulated. As shown from previous in Figure 3.1, the primary step of the proposed RMPA design process is the design of the RMPA with maximum frequency (i.e., 29GHz). In order to do that the MATLAB software with the set of the following equations are utilised [22]:

$$W_{patch} = \frac{3 \times 10^8}{2f_r\sqrt{\frac{(\varepsilon_r + 1)}{2}}} \tag{3.1}$$

$$\varepsilon_{reff} = \frac{\varepsilon_r + 1}{2} + \frac{\varepsilon_r - 1}{2}\left[1 + 12\frac{h}{W}\right]^{\frac{-1}{2}} \tag{3.2}$$

$$\Delta L = 0.412h\frac{\left(\varepsilon_{reff} + 0.3\right)\left[\frac{W_{patch}}{h} + 0.264\right]}{\left(\varepsilon_{reff} - 0.258\right)\left[\frac{W_{patch}}{h} + 0.8\right]} \tag{3.3}$$

$$L_{eff=}\frac{3 \times 10^8}{2f_r\sqrt{\varepsilon_{reff}}} \tag{3.4}$$

$$L_{patch} = L_{eff} - 2\Delta L \tag{3.5}$$

$$f_i = \frac{\cos^{-1}\left(\sqrt{\frac{Z_o}{R_{in}}}\right)}{\frac{\pi}{L}} \tag{3.6}$$

$$B = \frac{377\pi}{2Z_0\sqrt{\varepsilon_r}} \tag{3.7}$$

$$W_{feed} = \frac{2h}{\pi}\left\{B - 1 - \ln(2B-1) + \frac{\varepsilon_r - 1}{2\varepsilon_r}\left[\ln(B-1) + 0.39 - \left(\frac{0.61}{\varepsilon_r}\right)\right]\right\} \tag{3.8}$$

$$L_{feed} = 3.96 \times W_{feed} \tag{3.9}$$

$$G_{pf} = \frac{3 \times 10^8 \times 4.65 \times 10^{-9}}{f_r\sqrt{2\varepsilon_{reff}}} \tag{3.10}$$

$$W_s = 2 \times W_{patch} \tag{3.11}$$

$$L_s = 2 \times L_{patch} \tag{3.12}$$

Where:

ε_{reff}: is referred to the effective dielectric constant;

W_{patch}: is refers to the width of the antenna patch;

L_{eff}: is refers to the effective length of the patch;

L_{patch}: is refers to the actual patch length;

ΔL: is refers to the length's extension;

Z_o: is refers to the equivalent to the feed line impedance;

R_{in}: is refers to the resonant input resistance;

W_{feed}: is refers to the feed line width;

L_{feed}: is refers to the feed line length;

G_{pf}: is refers to the distance between the feed and patch;

W_s: is refers to the width of the substrate, and

L_s: is refers to the length of the substrate.

After completion of the calculation of the RMPA dimensions via the MATLAB® code, the simulation operation via the CST is started. The ground plane, substrate, antenna patch, and feeding line dimensions of the RMPA are summarised in Table 3.2.

Table 3.2: Dimensions of the RMPA.

Parameter	**Calculated Model (mm)**	**Modified Value (mm)**
W_{patch}	4.0892	4.03
L_{patch}	3.4405	3.33
f_{inset}	1.1668	0.9
W_{feed}	0.3107	0.3
L_{feed}	2.83	2.83
G_{pf}	0.2	0.2

The final shape of the simulated RMPA in the CST software is presented in Figure 3.2; the parts of the patch, feed line, and distance between them described in Figure 3.3.

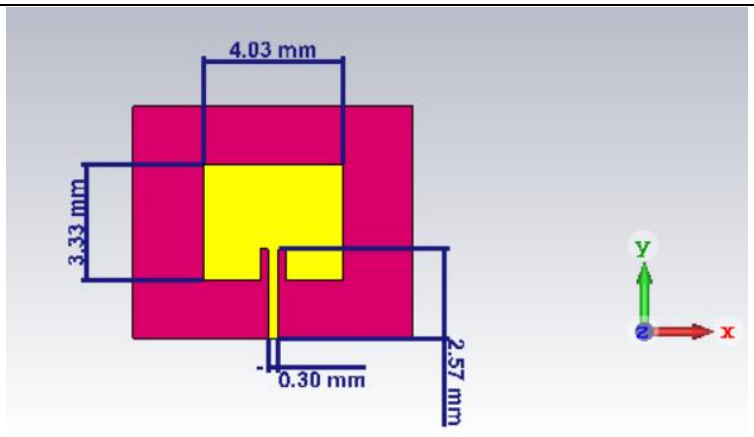

Figure 3.2: RMPA in CST.

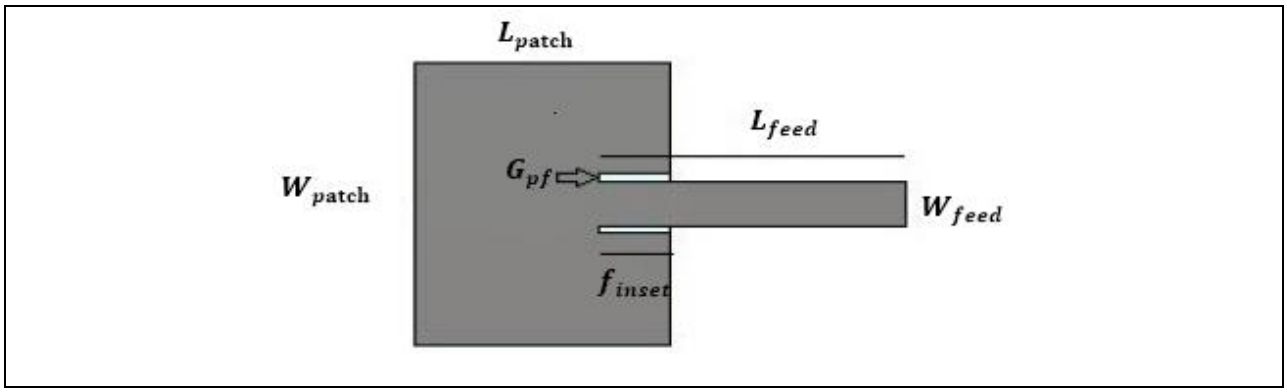

Figure 3.3: Patch and Feed Line Configuration.

3.3 RECONFIGURABLE RMPA DESIGN

To illustrate the utilisation of the graphene material in the reconfigurable antennas, the primary studied design is an RMPA which is made up from a combination of the copper patch with implanted graphene flakes inside it. The following step for the design procedure is the selection of the graphene flakes' positions on the patch by observing the distribution of the surface current on the patch and later, decide the proper positions of the moderate current density accumulation. In this work, the one most of the abnormal features that characterised the graphene material is employed which is the variable surface impedance that linked with the applied DC voltage (Va). Whereas the graphene flakes (i.e., implanted slots) work as a voltage-controlled switch to controlling the distribution of the current over the patch. When the Va raises the impedance of the graphene flakes drops and allowed the current to pass through it, on the other hand, once the Va drops the flakes impedance raised and just the leakage currents pass through it. These switching states lead to making the patch of the antenna in the normal size in the ON state (i.e., high Va) and smaller than its real size in the OFF state (i.e., small Va). This lead to creating an antenna able to working in multiple frequencies according to the ON or OFF state, Figure 3.4 presents the distribution of the current over the antenna patch.

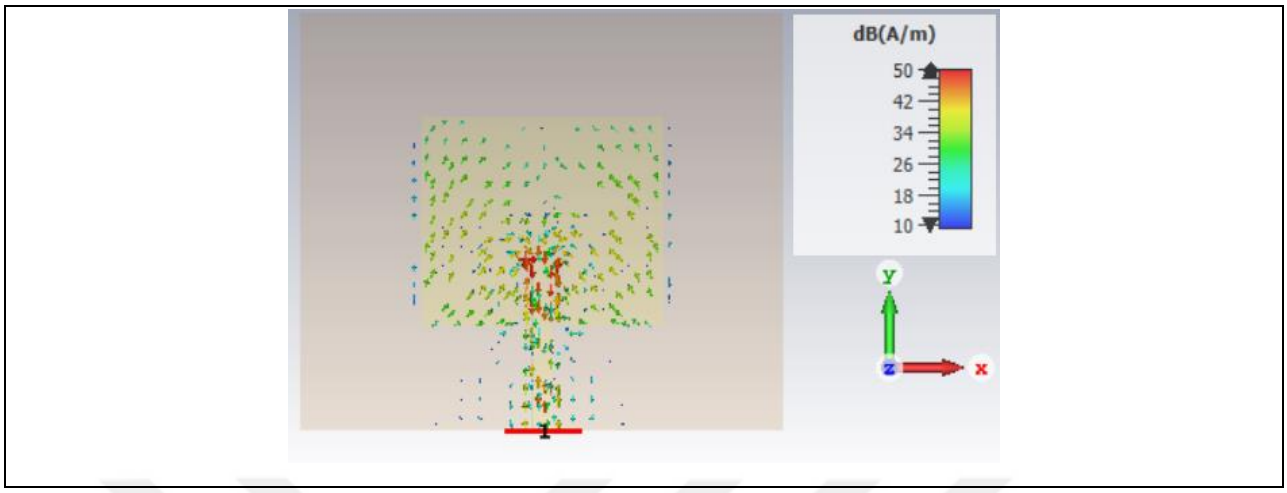

Figure 3.4: Current Distribution on The Patch of the Base Antenna.

After checking the current distribution on the patch, two graphene flakes with a dimensions of (0.1×0.3 mm) are implanted on the left and right middle edge of the patch within the place of the good current distribution to avoid the high value of the signal reflection, as illustrated in Figure 3.5. The value of the Va could be practised immediately to the graphene flakes this can be done through the antenna feeding port. In order to model the graphene material in the CST® software, the flakes impedance is calculated via the MATLAB® software by utilising the set of the equations that previously mentioned in section (2.10.3). The value of the impedance of the graphene flakes is determined by variating the charge carriers' density (i.e., minimising or maximising) as demonstrated in equation (2.11). Table 3.3 summarises the chosen and calculated values of the parameters of the graphene flakes impedance for the both ON/OFF states, (where the constant values are selected according to [31].

Table 3.3: Selected Parameters for Graphene Material Modelling.

Parameter	**Description**	
Case	Case #1: "ON"	Case #2: "OFF"
μ_l(m^2/Vs)	2.7	
D (eV)	4	
d	10nm	
T (K)	295	295
V_a (V)	40V	"~0"
$Z_S(\Omega)$	6 + 1.8i	1210.6+27.3i

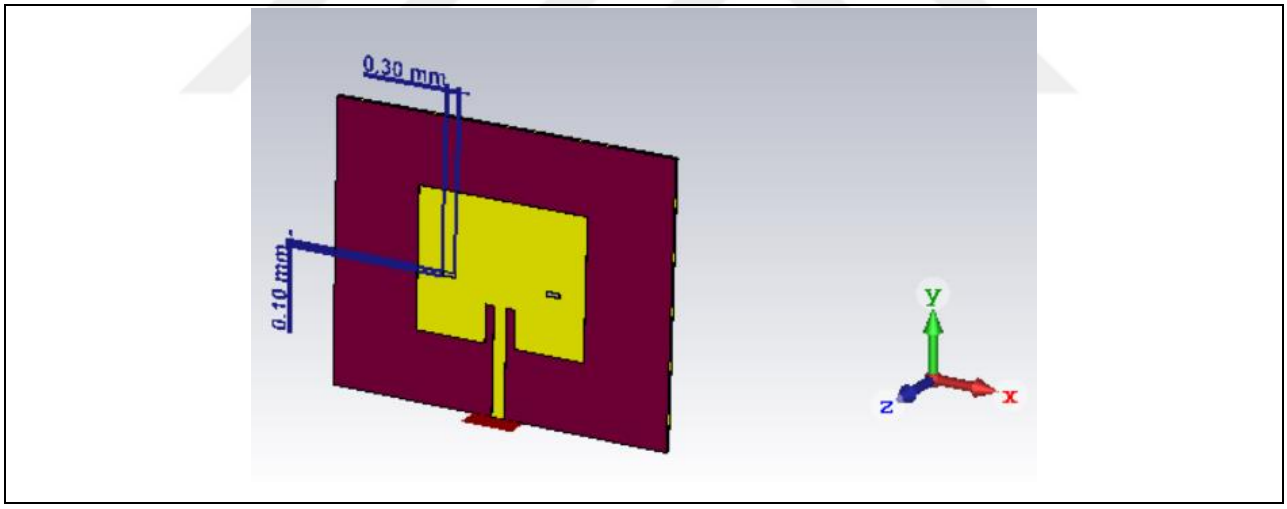

Figure 3.5: Proposed Reconfigurable Graphene-Based RMPA.

Once the proposed graphene-based RMPA simulation is completed, a surface current monitor is creating to observe the current distribution on the patch in the both ON and OFF cases. In the ON case, the current is able to pass through the flake due to the small impedance, contrary in the OFF state the current isn't able to pass due to the high impedance value and only the leakage current is present on the flakes, as shown in Figure 3.6.

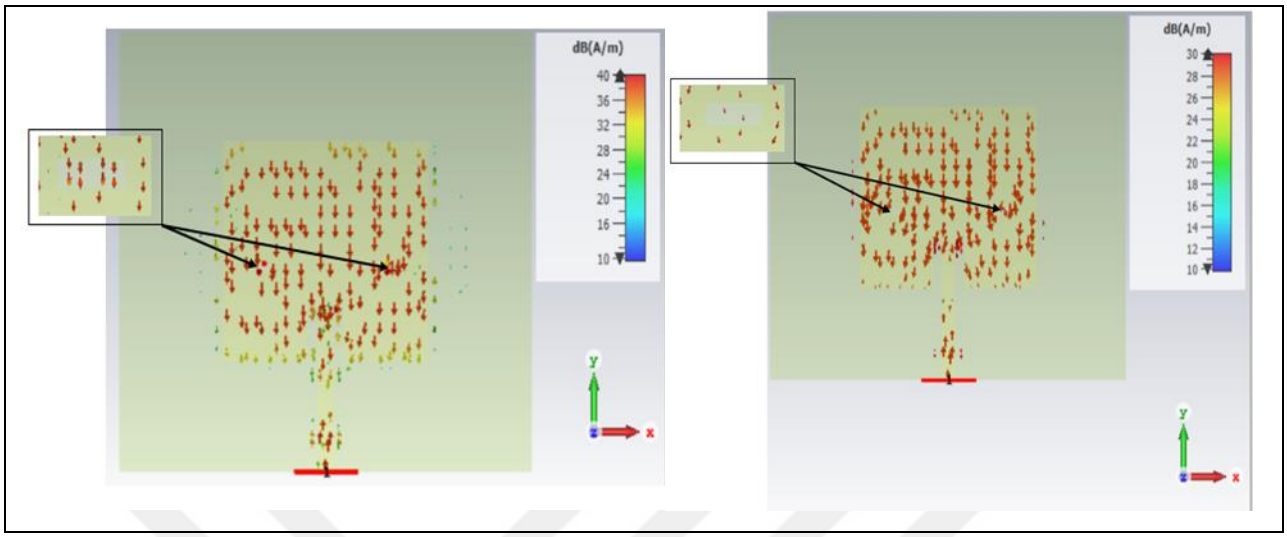

(a) ON Case (b) OFF case

Figure 3.6: The Graphene Flakes in the ON/OFF Cases.

3.4 OBTAINED RESULTS FOR RECONFIGURABLE RMPA

The following sections present the obtained results from the CST software for the proposed reconfigurable RMPA; such as S_{11}, BW, and antenna gain.

3.4.1 Results for S_{11}

The reversal of the power from the antenna comparable to the transmitted power to it is called the return loss (S_{11}). Thus, it required to stay as possible small, this meaning the antenna possesses approximately the most significant amount of the transmitted power. In general, the theories and the antenna designers introduced the $S_{11} = -10$ dB criteria which mean 10% of the power is reflecting back toward the source direction and the rest is received by the antenna. The obtained S_{11} results from the CST for proposed RMPA at the ON case is about (-31.37 dB) and (-37.516 dB) for the OFF case, as presented in Figure 3.7 and 3.8.

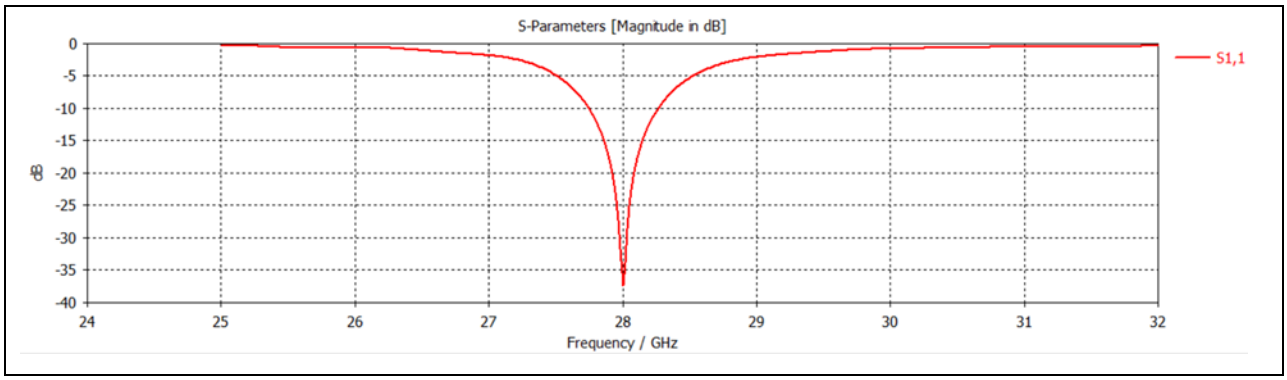

Figure 3.7: S_{11} Results for The Proposed Reconfigurable RMPA. on Case, $f_o = 29.12GHz$

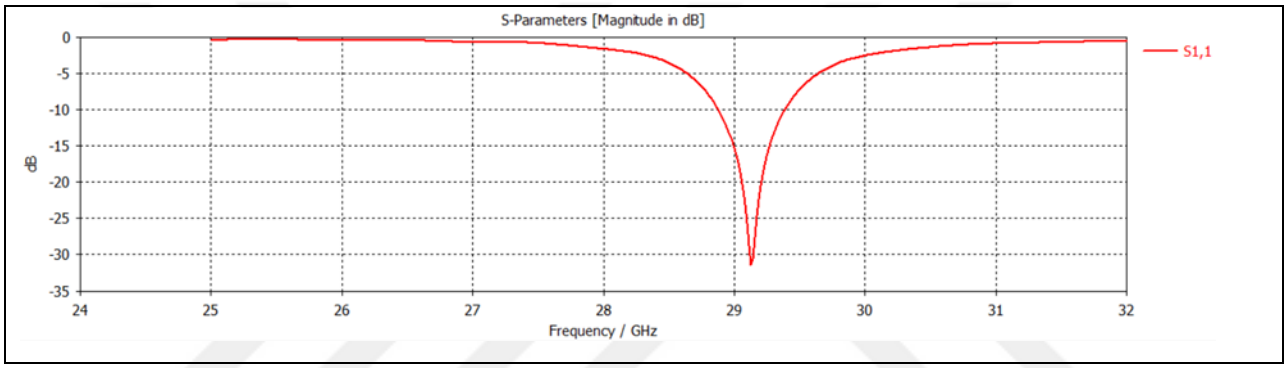

Figure 3.8: S_{11} Results for The Proposed Reconfigurable RMPA. off Case, $f_o = 28GHz$

3.4.2 Results for BW

The antenna BW refers to the range over which the antenna will operate properly with good performance. The antenna BW can be determined by utilising the S_{11} pattern. The obtained BW results from the CST for proposed reconfigurable RMPA at the ON case is about (503.53 MHz) and (523.41 MHz) for the OFF case, as presented in Figure 3.9 and 3.10.

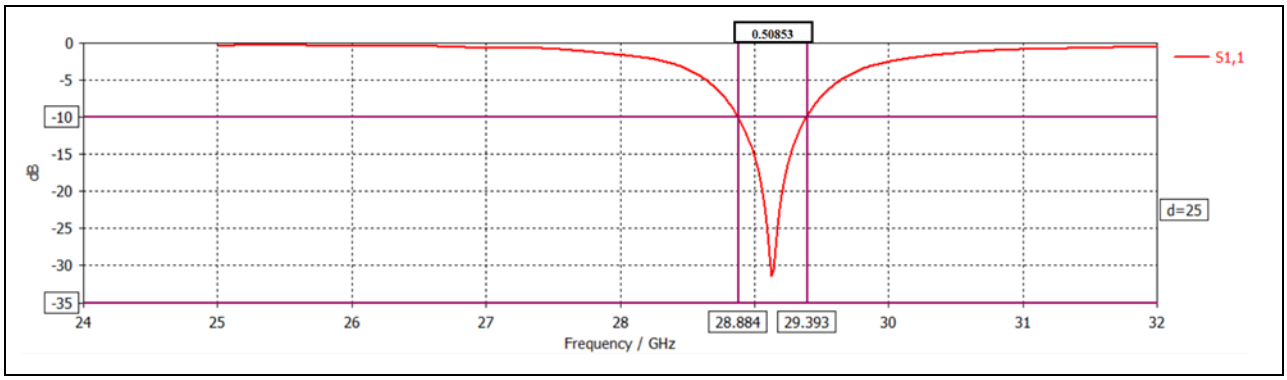

Figure 3.9: BW Results for the Proposed Reconfigurable RMPA. on Case, $f_o = 29.12GHz$

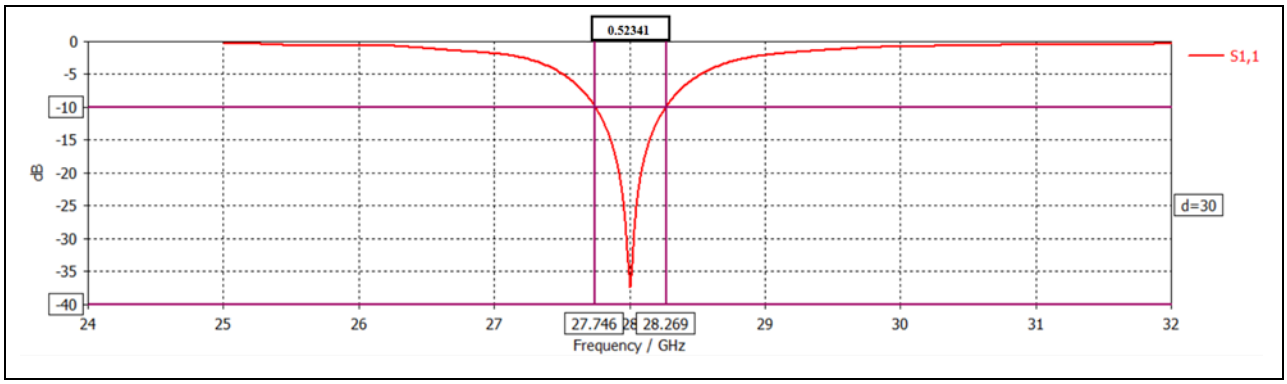

Figure 3.10: BW Results for the Proposed Reconfigurable RMPA.off Case, $f_o = 28GHz$

3.4.3 Results for Antenna Gain

The gain of the MPA generally is poor, because it's affected by the dielectric material thickness and relative permittivity constant. The obtained gain results from the CST for proposed reconfigurable RMPA at the ON case is about (6.12dBi) and (4.99dBi) for the OFF case, as presented in Figure 3.11 and 3.12.

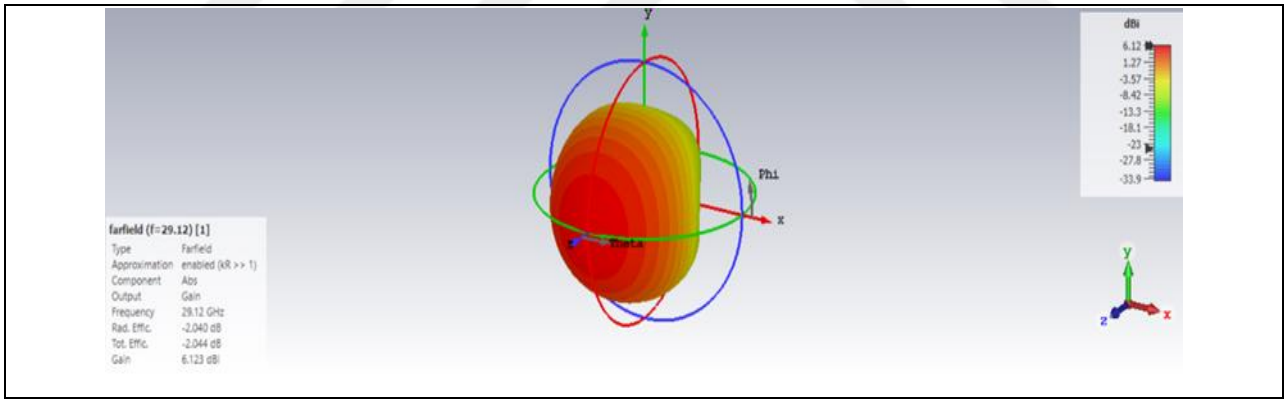

Figure 3.11: Gain Results for The Proposed Reconfigurable RMPA. on Case, $f_o = 29.12GHz$

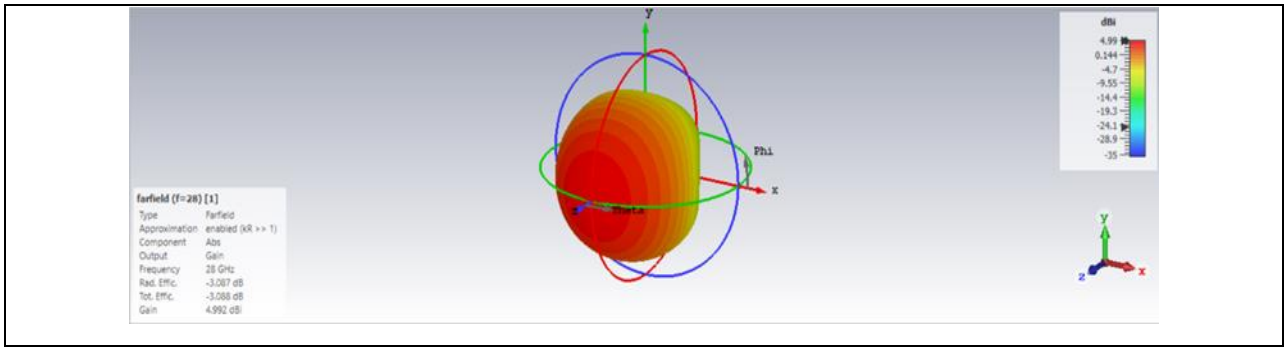

Figure 3.12: Gain results for the proposed reconfigurable RMPA. off Case, $f_o = 28GHz$

3.5 RECONFIGURABLE RMPAA DESIGN

As mentioned in the previous studies the MPA has a poor gain because of the presence of the substrate. Many methods are utilised to improve its gain, in our work the array configuration with a corporate feed is utilised. The design process is generally based on the "Antenna Magus®" software that helps us to export the 4×1 MPAA structure completely. Figure 3.10 illustrates the MPAA after exported from the "Antenna Magus" software and remove its original patches to be in the CST environment.

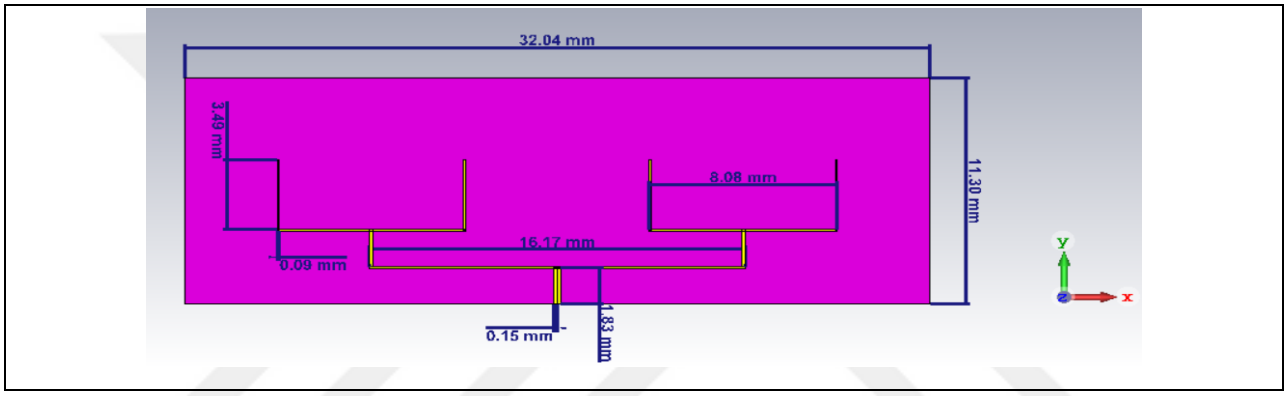

Figure 3.13: Corporate feed for 4×1 array.

After that, the array elements (i.e., imported patches) are removed and copy-paste the previous RMPA design to be the elements for the MPAA, as shown in Figure 3.14. The corporate feed is preferred to be utilised because the current is split in an equal manner for each element, thus contributes to a performance improvement.

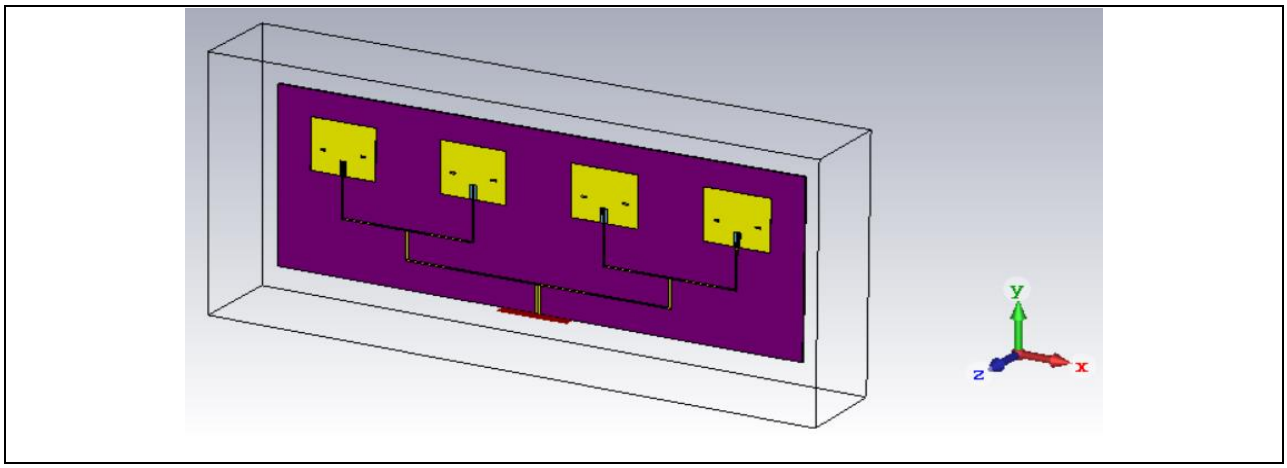

Figure 3.14: Proposed Reconfigurable RMPA.

3.6 RESULTS FOR THE RECONFIGURABLE RMPA

The following sections present the obtained results from the CST software for the proposed reconfigurable RMPA; such as S_{11}, BW, and antenna gain.

3.6.1 Results for S_{11}

Due to the presence of the feed network, the copper losses are increased and the current distribution is different from that in the single RMPA so that the results for the RMPAA and the RMPA are dissimilar (i.e., there is a shift in the f_o). The obtained S_{11} results for the RMPAA in the ON is about (-19.72 dB) and about (-23.18 dB) in the OFF case, as shown in Figure 3.15 and 3.16.

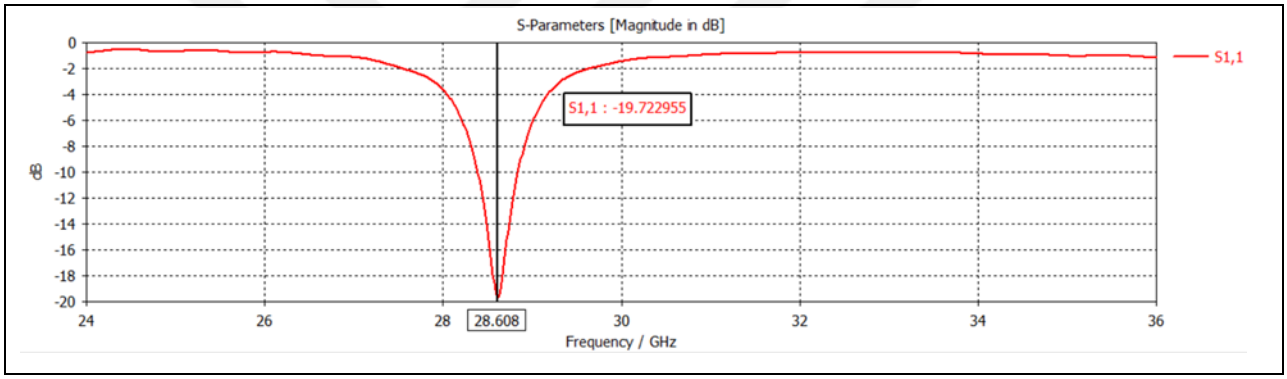

Figure 3.15: The S_{11} results for the proposed reconfigurable RMPA. on Case, $f_o = 28.608GHz$

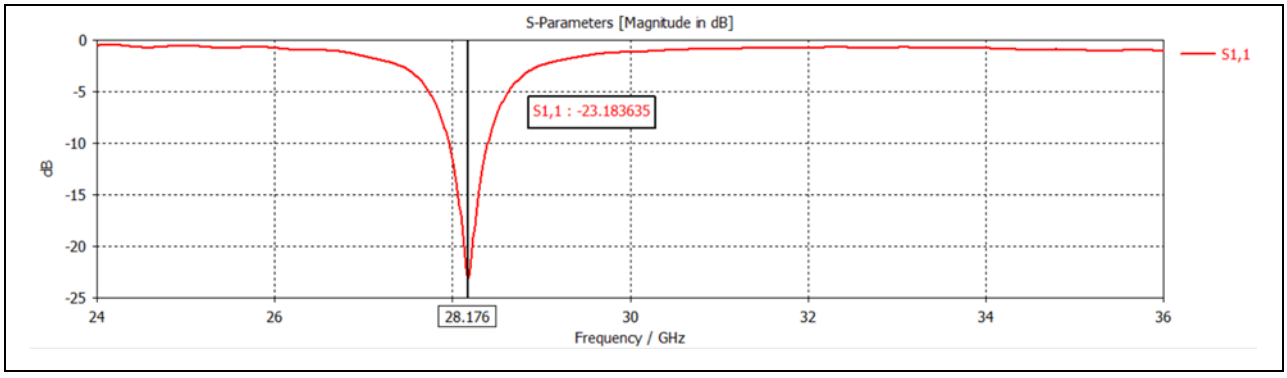

Figure 3.16: The S_{11} results for the proposed reconfigurable RMPA. off Case, $f_o = 28.176GHz$

3.6.2 Results for BW

The BW results for the proposed reconfigurable RMPA in the ON case is equal (453.43MHz) and (444.15MHz) in the OFF case, as illustrated in Figure 3.17 and 3.18.

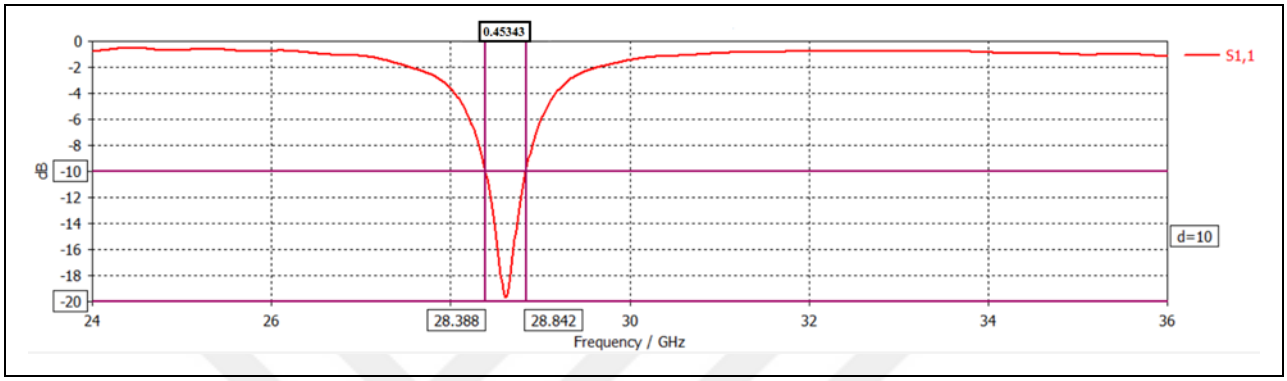

Figure 3.17: The BW Results for the Proposed Reconfigurable RMPAA. on Case, $f_o = 28.608GHz$

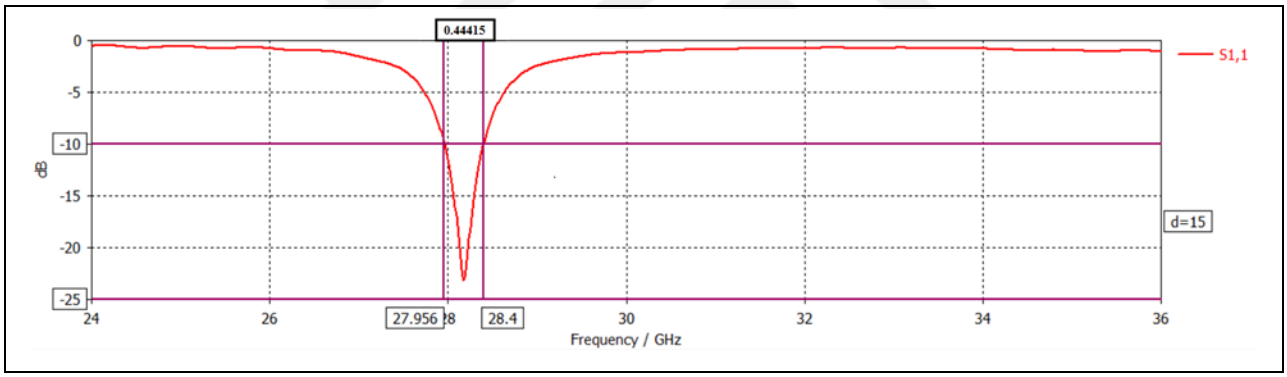

Figure 3.8: The BW Results for the Proposed Reconfigurable RMPAA. off Case, $f_o = 28.176GHz$

3.6.3 Results for Antenna Gain

In order to demonstrate the gain enhancement in the case of the array configuration, we compare the results at $f_o = 28$ GHz. The obtained gain result at the mentioned frequency equals (11 dBi), which does mean the gain approximately increased by (6 dBi) than the case of the utilisation of the single RMPA, as shown in Figure 3.19.

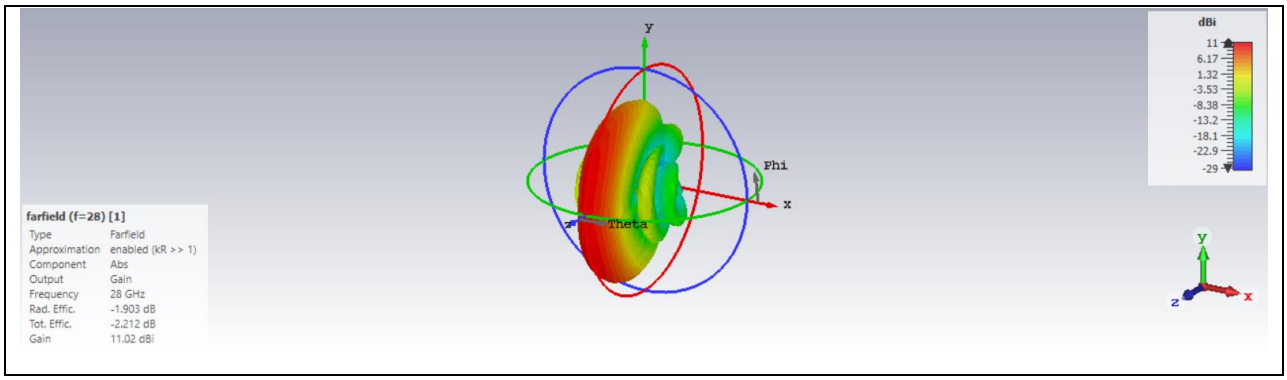

Figure 3.9: Gain for the Proposed Reconfigurable RMPAA at 28GHz.

After that, we monitor the gain of the proposed reconfigurable RMPAA in the both ON and OFF cases to be equal to (11.1 dBi) which are similar in both, as presented in Figure 3.20 and 3.21.

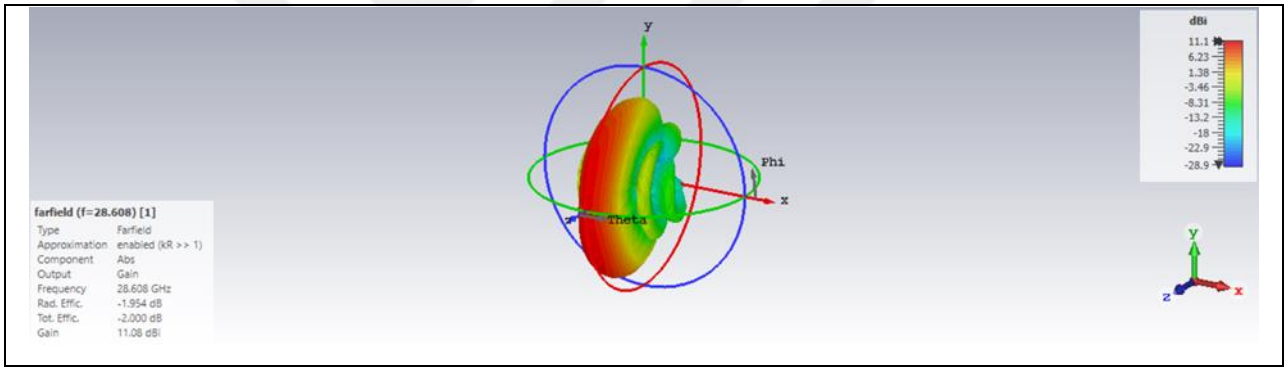

Figure 3.20: Gain Results for the Proposed Reconfigurable RMPAA. on Case, $f_o = 28.608GHz$

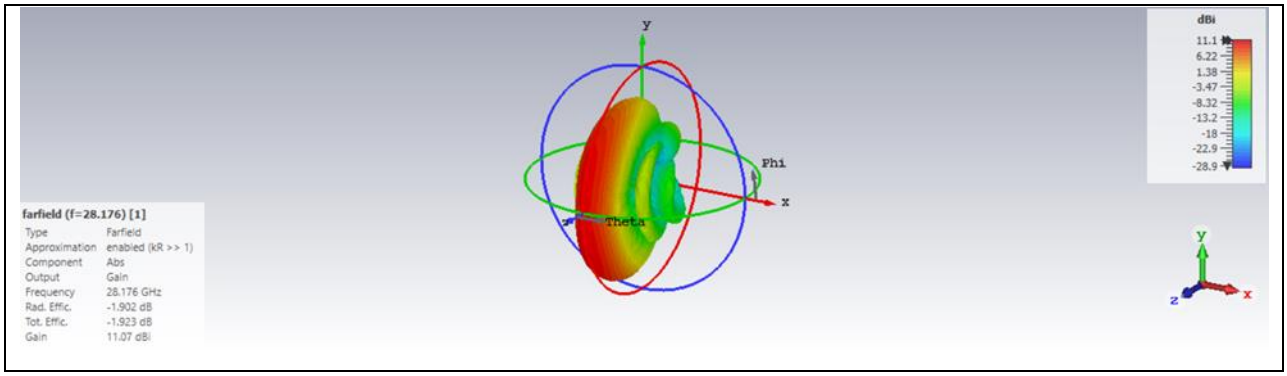

Figure 3.21: Gain Results for the Proposed Reconfigurable RMPAA. off Case, $f_o = 28.176GHz$

In the case of the reconfigurable RMPAA we note that the gain of the antenna is enhanced at 28GHz approximately by (6 dBi) and as the array elements increased the gain is enhanced also.

4. CONCLUSION AND FUTURE WORK

4.1 CONCLUSION

In this study, frequency reconfigurable RMPA and RMPAA have been designed as well as simulated based on the CST software. The radiated patch of the proposed RMPA is entirely designed from the copper with two flakes of the graphene material sowed within it. The graphene flakes have a variable surface impedance related to the applied V_a that help to shift the frequency. The proposed reconfigurable RMPA is operated in a frequency range of about (27.75- 29.4 GHz) with a gain (6.12-4.99 dBi). In addition, to enhance the antenna gain the RMPAA was utilised in this study which helps to enhance the gain by (6 dBi). The utilised RMPAA was based on the corporate feeding techniques that split the current equally for each element, which was designed through the "Antenna Magus" software. Because of the presence of the feeding network in the RMPAA, the copper losses increased which lead to variation the current distribution, finally, we noted the centre frequency in the ON/OFF cases is differing from that of the RMPA to be in the range of (27.95-28.84 GHz).

4.2 FUTURE ADVICE

In order, to develop the simulated reconfigurable RMPA/RMPAA many of modifications could be applied in the future, some of which can be summarised as the following:

a) Fabricate, test, and measure the simulated designs

b) Increase the number of the elements in the RMPAA to enhance the gain

c) Utilise the meta-material structures to enhance the overall antenna performance

d) Enhance the RMPAA performance by minimising the mutual coupling among the elements by utilising the electromagnetic bandgap structures.

REFERENCES

[1] Schrick, B., & Riezenman, M. J., "Wireless broadband in a box", IEEE Spectrum, vol.39, no.6, pp.38-43, 2002.

[2] Akyildiz, I. F., Wang, X., & Wang, W., "Wireless mesh networks: a survey", Computer networks, vol. 47, no. 4, pp. 445-487, 2005.

[3] Agrawal, J., Patel, R., Mor, P., Dubey, P., & Keller, J. M., "Evolution of mobile communication network: From 1G to 4G", International Journal of Multidisciplinary and Current Research, vol. 3, pp. 1100-1103, 2015.

[4] Brand, A., & Aghvami, H., "Multiple access protocols for mobile communications: GPRS, UMTS and beyond", John Wiley & Sons, 2002.

[5] Mehta, H., Patel, D., Joshi, B., & Modi, H., "0G to 5G mobile technology: a survey", J. of Basic and Applied Engineering Research, vol.1, no.6, pp. 56-60, 2015.

[6] Ali, M. F., Jayakody, D. N. K., Chursin, Y. A., Affes, S., & Dmitry, S., "Recent advances and future directions on underwater wireless communications", Archives of Computational Methods in Engineering, vol.27, no.5, pp.1379-1412, 2020.

[7] Alsharif, M. H., & Nordin, R., "Evolution towards fifth-generation (5G) wireless networks: Current trends and challenges in the deployment of millimetre wave, massive MIMO, and small cells", Telecommunication Systems, vol. 64, no.4, pp. 617-637, 2017.

[8] Abdullah, Q., Abdullah, N., Balfaqih, M., Shah, N. S. M., Anuar, S., Almohammedi, A. A., & Shepelev, V., "Maximising system throughput in wireless powered sub-6 GHz and millimetre-wave 5G heterogeneous networks", Telkomnika, vol.18, no.3, pp. 1185-1194, 2020.

[9] Uwaechia, A. N., & Mahyuddin, N. M., "A comprehensive survey on millimeter wave communications for fifth-generation wireless networks: Feasibility and challenges", IEEE Access, vol.8, pp. 62367-62414, 2020.

[10] Lecci, M., Testolina, P., Polese, M., Giordani, M., & Zorzi, M., "Accuracy vs. Complexity for mmWave Ray-Tracing: A Full Stack Perspective", IEEE Transactions on Wireless Communications, vol. 17, pp.1-16, 2021.

[11] Ram, N., Gao, H., Qin, H., Oo, M. T., & Htun, Y. T., "Statistical Channel Modelling of Millimetre Waves at 28 GHz and 73 GHz Frequency Signals Using MIMO Antennas", In Journal of Physics: Conference Series, IOP Publishing, vol. 1732, no. 1, pp. 1-8, 2021.

[12] Abu-Ella, O., Anairia, A., & Zubia, M., "Pathloss Modelling for Next Generation of Millimeter-Wave Communications", In 2021 IEEE 1st International Maghreb Meeting of the Conference on Sciences and Techniques of Automatic Control and Computer Engineering MI-STA, pp. 776-781, 2021.

[13] Marcus, M., & Pattan, B., "Millimeter wave propagation: spectrum management implications", IEEE Microwave Magazine, vol. 6, no.2, pp. 54-62, 2005.

[14] Mizuno, K., Matono, H., Wagatsuma, Y., Warashina, H., Sato, H., Miyanaga, S., & Yamanaka, Y., "New applications of millimeter-wave incoherent imaging", In IEEE MTT-S International Microwave Symposium Digest, IEEE, pp. 629-632, 2005.

[15] Sahoo, B. P., Chou, C. C., Weng, C. W., & Wei, H. Y., "Enabling millimeter-wave 5G networks for massive IoT applications: A closer look at the issues impacting millimeter-waves in consumer devices under the 5G framework", IEEE Consumer Electronics Magazine, vol.8, no.1, pp. 49-54, 2018.

[16] Bisognin, A., Arboleya, A., Titz, D., Pilard, R., Gloria, D., Gianesello, F., & Luxey, C., "Low-cost organic-substrate module for Tx-Rx short-range WiGig Communications at 60 GHz", IEEE Transactions on Antennas and Propagation, 2021.

[17] Aishah, A. S., Mohd Rashidi, C. B., Norlyana, S., & Syed Alwee Aljunid, S. J., "60 GHz milimeter-wave antennas for point-to-point 5G communication system", MATEC Web of Conferences, vol. 140, pp. 1-4, 2017.

[18] Moradi, K., Pourziad, A., & Nikmehr, S., "A frequency reconfigurable microstrip antenna based on graphene in Terahertz Regime" Optik, vol. 228, pp. 166201, 2021.

[19] Zhu, H. L., Cheung, S. W., Liu, X. H., Cao, Y. F., & Yuk, T. I., "Frequency reconfigurable antenna using metasurface", IEEE Transaction on antenna and propagation, vol. 62, no. 1, pp. 80-85, 2014.

[20] Bhattacharya, A., & Jyoti, R., "Frequency reconfigurable patch antenna using PIN diode at X-band", In 2015 IEEE 2nd international conference on recent trends in information systems (ReTIS), pp. 81-86, 2015.

[21] Yasir, M., Savi, P., Bistarelli, S., Cataldo, A., Bozzi, M., Perregrini, L., & Bellucci, S., "A planar antenna with voltage-controlled frequency tuning based on few-layer graphene", IEEE Antennas and wireless propagation Letters vol.16, pp. 2380-2383, 2017.

[22] Stutzman, W. L., & Thiele, G. A., "Antenna theory and design", John Wiley & Sons, 2012.

[23] Milligan, T. A., "Modern antenna design", John Wiley & Sons, 2005.

[24] Yaghjian, A. D., & Best, S. R., "Impedance, bandwidth, and Q of antennas", IEEE Transactions on Antennas and Propagation, vol.53, no.4, pp. 1298-1324, 2005.

[25] Bisht, S., Saini, S., Prakash, V., & Nautiyal, B., "Study the various feeding techniques of microstrip antenna using design and simulation using CST microwave studio", International Journal of Emerging Technology and Advanced Engineering, vol.4, no.9, pp. 318-324, 2014.

[26] Khraisat, Y. S., & Olaimat, M. M., "Comparison between rectangular and triangular patch antennas array", In 2012 19th International Conference on Telecommunications (ICT),IEEE, pp. 1-5, 2012.

[27] Hader, G. G., "Synthesis of graphene", In Synthesis, Modeling, and Characterization of 2D Materials, and Their Heterostructures, Elsevier pp. 181-221, 2020 .

[28] Korkmaz, S., & Kariper, İ. A., "Graphene and graphene oxide based aerogels: Synthesis, characteristics and supercapacitor applications", Journal of Energy Storage, vol.27, pp.101038, 2020.

[29] Dhinakaran, V., Lavanya, M., Vigneswari, K., Ravichandran, M., & Vijayakumar, M. D., "Review on exploration of graphene in diverse applications and its future horizon", Materials Today: Proceedings, vol.27, pp.824-828, 2020.

[30] Abdulnabi, H. A., & Al-Aboosi, Y. Y., " Design of Tunable Multiband Hybrid Graphene Metal Antenna in Microwave Regime", Indonesian Journal of Electrical Engineering and Computer Science, vol. 12, no. 3, pp. 401-408, 2018.

[31] Alvarez, C. N., Cheung, R., & Thompson, J. S., "Performance analysis of hybrid metal–graphene frequency reconfigurable antennas in the microwave regime", IEEE Transactions on Antennas and Propagation, vol.65, no.4, pp. 1558-1569, 2017.